



**HAL**  
open science

## High aboveground carbon stock of African tropical montane forests

Aida Cuni-Sanchez, Martin J. P. Sullivan, Philip J. Platts, Simon L. Lewis, Rob Marchant, Gérard Imani, Wannes Hubau, Iveren Abiem, Hari Adhikari, Tomas Albrecht, et al.

► **To cite this version:**

Aida Cuni-Sanchez, Martin J. P. Sullivan, Philip J. Platts, Simon L. Lewis, Rob Marchant, et al.. High aboveground carbon stock of African tropical montane forests. *Nature*, 2021, 596 (7873), pp.536-542. 10.1038/s41586-021-03728-4 . hal-03329118

**HAL Id: hal-03329118**

**<https://hal.inrae.fr/hal-03329118>**

Submitted on 19 May 2022

**HAL** is a multi-disciplinary open access archive for the deposit and dissemination of scientific research documents, whether they are published or not. The documents may come from teaching and research institutions in France or abroad, or from public or private research centers.

L'archive ouverte pluridisciplinaire **HAL**, est destinée au dépôt et à la diffusion de documents scientifiques de niveau recherche, publiés ou non, émanant des établissements d'enseignement et de recherche français ou étrangers, des laboratoires publics ou privés.

University of Dundee

## High aboveground carbon stock of African tropical montane forests

Cuni-Sanchez, Aida; Sullivan, Martin J. P.; Platts, Philip J.; Lewis, Simon L.; Marchant, Rob; Imani, Gérard

*Published in:*  
Nature

*DOI:*  
[10.1038/s41586-021-03728-4](https://doi.org/10.1038/s41586-021-03728-4)

*Publication date:*  
2021

*Document Version*  
Peer reviewed version

[Link to publication in Discovery Research Portal](#)

### *Citation for published version (APA):*

Cuni-Sanchez, A., Sullivan, M. J. P., Platts, P. J., Lewis, S. L., Marchant, R., Imani, G., Hubau, W., Abiem, I., Adhikari, H., Albrecht, T., Altman, J., Amani, C., Aneseyee, A. B., Avitabile, V., Banin, L., Batumike, R., Bauters, M., Beeckman, H., Begne, S. K., ... Zibera, E. (2021). High aboveground carbon stock of African tropical montane forests. *Nature*, 596(7873), 536-542. <https://doi.org/10.1038/s41586-021-03728-4>

### **General rights**

Copyright and moral rights for the publications made accessible in Discovery Research Portal are retained by the authors and/or other copyright owners and it is a condition of accessing publications that users recognise and abide by the legal requirements associated with these rights.

- Users may download and print one copy of any publication from Discovery Research Portal for the purpose of private study or research.
- You may not further distribute the material or use it for any profit-making activity or commercial gain.
- You may freely distribute the URL identifying the publication in the public portal.

### **Take down policy**

If you believe that this document breaches copyright please contact us providing details, and we will remove access to the work immediately and investigate your claim.

## 1 High above-ground carbon stock of African tropical montane forests

2  
3 Aida Cuni-Sanchez<sup>1,2\*</sup>, Martin J.P. Sullivan<sup>3,4</sup>, Phil J. Platts<sup>1,5</sup>, Simon L. Lewis<sup>4,6</sup>, Rob Marchant<sup>1</sup>, Gérard  
4 Imani<sup>7</sup>, Wannes Hubau<sup>8,9</sup>, Iveren Abiem<sup>10,11</sup>, Hari Adhikari<sup>12</sup>, Tomas Albrecht<sup>13,14</sup>, Jan Altman<sup>15</sup>,  
5 Christian Amani<sup>7</sup>, Abreham B. Aneseyee<sup>16,17</sup>, Valerio Avitabile<sup>18</sup>, Lindsay Banin<sup>19</sup>, Rodrigue  
6 Batumike<sup>20</sup>, Marijn Bauters<sup>21</sup>, Hans Beeckman<sup>8</sup>, Serge K. Begne<sup>4,22</sup>, Amy C. Bennett<sup>4</sup>, Robert  
7 Bitariho<sup>23</sup>, Pascal Boeckx<sup>21</sup>, Jan Bogaert<sup>24</sup>, Achim Bräuning<sup>25</sup>, Franklin Bulonvu<sup>26</sup>, Neil D. Burgess<sup>27</sup>,  
8 Kim Calders<sup>28</sup>, Colin Chapman<sup>29-31</sup>, Hazel Chapman<sup>11,33</sup>, James Comiskey<sup>34</sup>, Thales de Haulleville<sup>35</sup>,  
9 Mathieu Decuyper<sup>36,37</sup>, Ben DeVries<sup>38</sup>, Jiri Dolezal<sup>15,39</sup>, Vincent Droissart<sup>22,40</sup>, Corneille Ewango<sup>41</sup>,  
10 Senbeta Feyera<sup>42</sup>, Aster Gebrekirstos<sup>43</sup>, Roy Gereau<sup>44</sup>, Martin Gilpin<sup>4</sup>, Dismas Hakizimana<sup>45</sup>, Jefferson  
11 Hall<sup>46</sup>, Alan Hamilton<sup>47</sup>, Olivier Hardy<sup>48</sup>, Terese Hart<sup>49</sup>, Janne Heiskanen<sup>12,50</sup>, Andreas Hemp<sup>51</sup>, Martin  
12 Herold<sup>37,52</sup>, Ulrike Hiltner<sup>25,53</sup>, David Horak<sup>54</sup>, Marie-Noel Kamdem<sup>22</sup>, Charles Kayijamahe<sup>55</sup>, David  
13 Kenfack<sup>46</sup>, Mwangi J. Kinyanjui<sup>56</sup>, Julia Klein<sup>57</sup>, Janvier Lisingo<sup>41</sup>, Jon Lovett<sup>4</sup>, Mark Lung<sup>58</sup>, Jean-Remy  
14 Makana<sup>59</sup>, Yadvinder Malhi<sup>60</sup>, Andrew Marshall<sup>1,61,62</sup>, Emanuel H. Martin<sup>63</sup>, Edward T.A. Mitchard<sup>64</sup>,  
15 Alexandra Morel<sup>65</sup>, John T. Mukendi<sup>8</sup>, Tom Muller<sup>66</sup>, Felix Nchu<sup>67</sup>, Brigitte Nyirambangutse<sup>68,69</sup>,  
16 Joseph Okello<sup>21,70,71</sup>, Kelvin S.-H. Peh<sup>72,73</sup>, Petri Pellikka<sup>12,74</sup>, Oliver L. Phillips<sup>4</sup>, Andrew Plumptre<sup>75</sup>, Lan  
17 Qie<sup>76</sup>, Francesco Rovero<sup>77,78</sup>, Moses N. Sainge<sup>79</sup>, Christine B. Schmitt<sup>80,81</sup>, Ondrej Sedlacek<sup>54</sup>, Alain S.K.  
18 Ngute<sup>61,82</sup>, Douglas Sheil<sup>83</sup>, Demisse Sheleme<sup>84</sup>, Tibebu Y. Simegn<sup>85</sup>, Murielle Simo-Droissart<sup>22</sup>,  
19 Bonaventure Sonké<sup>22</sup>, Teshome Soromessa<sup>16</sup>, Terry Sunderland<sup>86,87</sup>, Miroslav Svoboda<sup>88</sup>, Hermann  
20 Taedoumg<sup>89,90</sup>, James Taplin<sup>91</sup>, David Taylor<sup>92</sup>, Sean C. Thomas<sup>93</sup>, Jonathan Timberlake<sup>94</sup>, Darlington  
21 Tuagben<sup>95</sup>, Peter Umunay<sup>96</sup>, Eustrate Uzabaho<sup>55</sup>, Hans Verbeeck<sup>28</sup>, Jason Vleminckx<sup>97</sup>, Göran Wallin<sup>69</sup>,  
22 Charlotte Wheeler<sup>64</sup>, Simon Willcock<sup>98,99</sup>, John T. Woods<sup>100</sup>, Etienne Zibera<sup>68</sup>

23

### 24 Abstract

25 Tropical forests store 40-50% of terrestrial vegetation carbon<sup>1</sup>. Spatial variations in aboveground live  
26 tree biomass carbon (AGC) stocks remain poorly understood, in particular in tropical montane  
27 forests<sup>2</sup>. Owing to climatic and soil changes with increasing elevation<sup>3</sup>, AGC stocks are lower in  
28 tropical montane compared to lowland forests<sup>2</sup>. Here we assemble and analyse a dataset of  
29 structurally intact old-growth forests (AfriMont) spanning 44 montane sites in 12 African countries.  
30 We find that montane sites in the AfriMont plot network have a mean AGC-stock of 149.4 Mg C ha<sup>-1</sup>  
31 (95% CI 137.1-164.2), comparable to lowland forests in the African Tropical Rainforest Observation  
32 Network<sup>4</sup> and about 70 per cent and 32 per cent higher than averages from plot networks in  
33 montane<sup>2,5,6</sup> and lowland<sup>7</sup> forests in the Neotropics, respectively. Notably, our results are two-thirds  
34 higher than the IPCC default values for these forests in Africa<sup>8</sup>. We find that the low stem density  
35 and high abundance of large trees of African lowland forests<sup>4</sup> is mirrored in the montane forests  
36 sampled. This carbon store is endangered: we estimate that 0.8 million ha of old-growth African  
37 montane forest have been lost since 2000. We provide country-specific montane forest AGC stock  
38 estimates modelled from our plot network to help guide forest conservation and reforestation  
39 interventions. Our findings highlight the need for conserving these biodiverse<sup>9,10</sup> and carbon-rich  
40 ecosystems.

41

42

43 **Main text**

44 Tropical forests cover less than 10% of the global land area yet store 40–50% of terrestrial  
45 vegetation carbon<sup>1</sup> and contribute more than one third of primary productivity<sup>11</sup> so are a key  
46 component of the global carbon cycle<sup>12,13</sup>. There is substantial variation in carbon stocks across the  
47 biome, with lowland forests in Africa and Borneo storing more carbon per unit area than lowland  
48 forests in the Neotropics<sup>4,7</sup>. This variation arises partly from structural differences: the signature  
49 feature of African forests is their low stem density but relatively high abundance of large trees (>70  
50 cm diameter) which store large quantities of carbon, while Bornean forests are characterised by high  
51 stem density and basal area<sup>4,14,15</sup>.

52

53 Despite increased understanding of biogeographic differences in tropical lowland forests, patterns of  
54 spatial variation in carbon stocks remain poorly understood in the 880,000 km<sup>2</sup> of tropical montane  
55 forests located  $\geq 1,000$  m asl<sup>2</sup>. Montane forests are expected *a priori* to have lower aboveground live  
56 tree biomass carbon (AGC) stocks than lowland forests because (1) temperature decreases with  
57 increasing elevation, reducing net primary productivity and slowing nutrient recycling, (2) long  
58 periods of cloud immersion in montane forests suppresses productivity, (3) soil waterlogging slows  
59 nutrient recycling and (4) high epiphyte load, local wind exposure in crests and nutrient-limited soils  
60 limit tree size and increase investment in roots over shoots<sup>3</sup>. While forest inventory plots provide  
61 some support for these assumptions<sup>2</sup> data from African mountain regions are exceptionally sparse.  
62 Indeed, in the most recent IPCC guidelines, there is no specific AGC default value for old-growth  
63 montane forests in Africa: the value given of 89.3 Mg C ha<sup>-1</sup> is simply a mean of secondary and old-  
64 growth forests found  $\geq 1,000$  m asl<sup>8</sup>. Mountain areas also pose special challenges for remote-sensing  
65 approaches for estimating carbon stocks, as radar data are affected by geometric distortions<sup>16</sup> while  
66 steep slopes bias spaceborne LiDAR estimates towards overestimating canopy height<sup>17</sup>. These issues  
67 are reflected in the limited correlation between estimates of AGC-stocks at mountain locations from  
68 different recent remote-sensing derived carbon maps (Supplementary Information Table S1).

69

70 Better understanding of montane carbon stocks is important for many African countries, particularly  
71 in eastern Africa where montane forests represent most of the extant evergreen old-growth forest  
72 cover. Quantifying carbon stocks in these ecosystems is critical for estimating national carbon losses  
73 from deforestation and forest degradation<sup>18</sup>. Quantifying carbon stocks in old-growth montane  
74 forests also serves to constrain potential carbon uptake by restored natural forests, given the high  
75 commitment of most African nations to the Bonn Challenge effort to restore 150 million ha of  
76 degraded and deforested lands by 2020 (see Table 1), and 350 million by 2030.

77

78 Here we measured, compiled and analysed a new dataset of 226 plot inventories spanning 44 sites  
79 in 12 African countries, covering most major mountain regions on the continent (the “AfriMont”  
80 dataset). Plots range from 800 to 3,900 m asl to include submontane forests (800-1,000 m asl) in  
81 smaller mountains closer to the ocean<sup>19,20</sup>. For all plots, stem diameter and species were recorded  
82 for each tree  $\geq 10$  cm diameter at breast height (or above buttress) following standard methods<sup>21</sup>.  
83 Tree height was sampled in 23 montane sites, allowing variation in height-diameter allometry to be  
84 incorporated into the calculation of aboveground biomass. A total of 72,336 stems with diameter  
85  $\geq 10$  cm were measured. For each tree, we computed AGC (in Mg C ha<sup>-1</sup>) according to standard  
86 procedures (see methods).

87

88 We find that the mean plot-level AGC-stock across sampled African tropical montane forests is 149.4  
89 Mg C ha<sup>-1</sup> (95% confidence interval (CI) 137.1-164.2), two-thirds more than the IPCC default value of  
90 89.3 Mg C ha<sup>-1</sup>. Our estimates are robust to subsampling our dataset (Extended Data Fig. 1) and  
91 excluding small plots (Extended Data Fig. 2) and are not affected by the sampling strategy used to  
92 establish plots in each study site (Extended Data Fig. 2). Comparing our dataset to previous  
93 syntheses of montane<sup>2,5,6</sup> and lowland<sup>7</sup> forest plot networks reveals that tropical montane forests in

94 Africa have significantly higher AGC-stocks per unit area than both montane (95% CI = 50.4 – 71.9  
95 Mg C ha<sup>-1</sup>) and lowland (95% CI = 124.0 – 147.9 Mg C ha<sup>-1</sup>) forests in the Neotropics, and that they  
96 do not differ significantly from lowland forests in Africa (95% CI = -27.6 – 9.6 Mg C ha<sup>-1</sup>) (Fig. 1, Table  
97 S2). The similar AGC-stocks in montane and lowland forests in Africa contrasts with the Neotropics  
98 and Southeast Asia, where carbon stocks are lower in montane forests than lowland forests (albeit  
99 not significantly different in Southeast Asia due to the small sample size, Fig. 1). These differences  
100 are robust to accounting for differences in elevation among montane datasets: removing African  
101 plots 800-1,000 m asl slightly reduces estimated montane forest AGC-stock to 145.0 Mg C ha<sup>-1</sup> (95%  
102 CI 129.6 – 163.2), but observed differences in AGC-stock among continents remain when plots are  
103 restricted to elevations well represented in all continents (Extended Data Fig. 3).

104

105 The characteristic structural properties of lowland African forests (relatively low stem density and  
106 greater importance of large trees compared to elsewhere in the tropics<sup>4</sup>) are also evident in the  
107 African montane forests we sampled. In these montane forests mean stem density is 483.3 stems ha<sup>-1</sup>  
108 ( $\pm 177.7$  s.d.) and mean basal area is 39 m<sup>2</sup>ha<sup>-1</sup> ( $\pm 14.8$  s.d.). We find a high density of large stems  
109 (>70 cm diameter, 19.1 stems ha<sup>-1</sup>  $\pm 15.4$  s.d.) which contribute 35.3% (95% CI = 29.6 – 41.8 %) to  
110 plot-level AGC-stock (Fig. 2). The contribution of large trees to plot-level AGC-stock is also similar in  
111 montane and lowland Africa (95% CI of difference in square-root transformed proportional  
112 contribution of large trees between lowland and montane forests = -0.100 - 0.075,  $P = 0.80$ ). There  
113 was no significant difference in the proportional contribution of any other size class to AGC-stocks  
114 between our montane dataset and 132 lowland plots from the AfriTRON network ( $P \geq 0.24$ , Table S3),  
115 although greater variation among plots is observed in montane forests (Fig. 2).

116

117 To investigate if elevation affected AGC or forest structure, we modelled these variables as functions  
118 of elevation using random slopes mixed-effects models. This approach allows intercepts and  
119 relationships to vary among sites, which would be expected as mountains can have very different  
120 climate at the same elevation due to proximity to the ocean (generally the further, the drier) and  
121 because of the mass-elevation or telescopic effect<sup>22</sup> (larger mountains are better at warming the  
122 atmosphere above them). We found that AGC, stem density or density of large stems (>70 cm  
123 diameter) were not significantly related to elevation (Fig. 3, Table S4). Across sites these non-  
124 significant relationships were all negative, although there was some variation in strength and  
125 direction amongst sites (Fig. 3). Similarly, in the Neotropics and Southeast Asia montane forest plot  
126 datasets, AGC was not significantly correlated with elevation (Extended Data Fig. 4).

127

128 To assess potential environmental drivers of AGC-stock variation across the AfriMont plot network,  
129 we related AGC to climate, soil and topography. We found that AGC-stocks increased with annual  
130 precipitation (albeit not statistically significantly), decreased with soil fertility and were higher in  
131 plots which were locally at higher elevation than their surroundings (Extended Data Fig. 5).  
132 Relationships with other environmental variables were non-significant (Extended Data Fig. 5).  
133 Although global datasets might not capture fine-scale variation in climate or soils in mountain  
134 regions<sup>23</sup>, leading to regression dilution<sup>24</sup>, the general absence of strong climate effects combined  
135 with the lack of significant effect of elevation on AGC-stocks suggest that the high AGC-stock of  
136 African montane forests is a pervasive phenomenon across a wide environmental gradient.

137

138 Although the AfriMont dataset covers most major mountain areas in tropical Africa (Fig. 4), some  
139 areas remain under-sampled relative to forest extents (Extended Data Fig. 6), resulting in some  
140 differences between the environmental conditions sampled by our plot network and the wider  
141 montane forest biome in Africa (Extended Data Fig. 7). Notably, the absence of plots from montane  
142 forests of eastern Democratic Republic of the Congo (Fig. 4, Extended Data Fig. 6) means that the  
143 AfriMont dataset samples forests are, on average, at higher elevations, and that are cooler and  
144 cloudier than the wider montane forest biome in Africa (Extended Data Fig. 7). Using relationships

145 with environmental variables (Extended Data Fig. 5) to predict AGC-stocks in each 1-km grid cell  
146 containing montane forest gives a mean (weighted by remaining forest cover) AGC-stock of 176.9  
147 Mg C ha<sup>-1</sup> ( $\pm$  32.0 s.d.) for the tropical montane forest biome in Africa. This indicates that the  
148 estimate we report based on our AfriMont plot network data (149.4 Mg C ha<sup>-1</sup>) is conservative.

149  
150 Several mechanisms could explain the high AGC-stock of montane forests in the AfriMont plot  
151 network. Firstly, large herbivores such as elephants (*Loxodonta* spp.) can have profound effects on  
152 forest structure by consuming biomass, destroying small stems, dispersing seeds and transporting  
153 nutrients<sup>25</sup>. Studies for lowland forests suggest that elephants can increase carbon stocks<sup>26,27</sup>. We  
154 tested if AfriMont plots with known elephant presence as of 2019 had significantly higher AGC-  
155 stocks, but found that they had significantly lower AGC-stocks, although significant differences were  
156 not observed in some countries (Extended Data Fig. 8). While the initial ecosystem response to  
157 elephant removal might be greater AGC-stocks due to reduced biomass consumption and small-stem  
158 destruction, the longer-term effects might differ. We were unable to fully disentangle such effects,  
159 as we lacked details on both i) time since elephant extirpation, and ii) elephant abundance and its  
160 determinants (see Table S5).

161  
162 A second potential explanation is a relatively low frequency of large-scale abiotic disturbances,  
163 allowing trees time to grow large and stands to self-thin, as is seen in lowland African forests<sup>4</sup>. For  
164 example, tropical cyclones are largely absent in mainland Africa (except in Mozambique<sup>28</sup>) and lava  
165 flows are limited even in the active volcano of Mt Cameroon<sup>29</sup>. Although fine-scale variability in  
166 landslide risk limits comparisons across large spatial scales, there are fewer areas with high landslide  
167 susceptibility in mountains in tropical Africa than in the Andes and most mountain ranges in  
168 Southeast Asia<sup>30</sup>. If forests have been ecologically stable over evolutionary timescales, tree species  
169 may be adapted to grow slowly but potentially reaching great sizes<sup>31</sup>. On Mt Kilimanjaro  
170 *Entandrophragma* individuals reach enormous heights and ages<sup>32</sup>. This low frequency of large-scale  
171 abiotic disturbances contrasts with the Andes and several mountains in Southeast Asia (e.g. Barisan  
172 mountains in western Sumatra), which are tectonically active, so the trees there are adapted to  
173 sudden disturbance followed by intense competition to get established and grow. Future monitoring  
174 of the AfriMont plot network will help determine the extent to which the high biomass of African  
175 tropical montane forests results from them being dynamic and productive, or adapted to stability.

176  
177 A third potential explanation could be the presence of conifers<sup>33</sup>. Mixed conifer/broad-leaved forests  
178 tend to have greater basal area than purely broad-leaved forests due to a more effective use of light  
179 and other resources<sup>34</sup>. Podocarpaceae can be found in montane forests across the tropics<sup>35</sup>. Despite  
180 having fewer species in Africa than in other continents<sup>36</sup>, these could be more abundant at the site-  
181 level. However, there is no pantropical comparative study on Podocarpaceae abundance in tropical  
182 montane forests. In our dataset there was no significant correlation between plot-level AGC-stock  
183 and conifer (Podocarpaceae) abundance (Extended Data Fig. 9). Other explanations could be  
184 continental differences in mountain terrain (more gentle slopes or plateau regions in Africa) or types  
185 of montane forests investigated (less cloud forest existing/sampled in Africa). Within our dataset,  
186 slope did not have a significant effect on AGC-stocks (Extended Data Fig. 5). Contrary to the  
187 Neotropics<sup>37</sup>, there is no high-resolution map of cloud forests available for Africa, so while we found  
188 no relationship between AGC-stock and cloud frequency (Extended Data Fig. 5), we were unable to  
189 investigate differences in AGC-stock between cloud forest vs non-cloud forest plots.

190  
191 To understand the policy implications of our findings for African countries, we calculated montane  
192 ( $\geq$ 800 m asl) forest cover change between 2000 and 2018, using forest cover from ref.<sup>38</sup> clipped to  
193 'primary humid forest' from ref.<sup>39</sup>. We show that tropical montane forests represent most -or all-  
194 evergreen old-growth forests found in ten African countries (Fig. 4), and that the Democratic  
195 Republic of the Congo has two thirds of the remaining 16 million ha of montane forests in Africa.

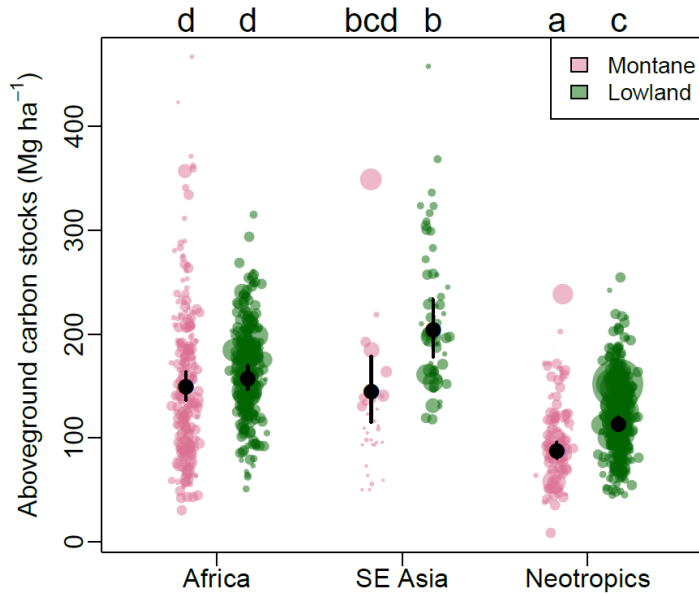
196 Over 0.8 million ha (5%) have been lost in Africa since 2001, with the highest losses in the  
197 Democratic Republic of the Congo (536,000 ha), Uganda (65,000 ha) and Ethiopia (62,000 ha) (Fig. 4,  
198 Table 1). In terms of percentage, Mozambique and Côte d'Ivoire lost over 20% of their montane  
199 forests over this period (Fig. 4, Table 1). In some sites, however, a larger proportion of montane  
200 forests was lost before 2000, e.g. in Taita Hills in Kenya<sup>40</sup>. If absolute country-level deforestation  
201 rates continue, a further 0.5 million ha of tropical montane forests will be lost by 2030.

202  
203 African tropical montane forests are not only carbon-rich, but they also harbour some of the highest  
204 concentrations of biodiversity and endemism in the world<sup>9,10</sup>. They are important 'water towers' as,  
205 located at the headwaters of numerous river systems, including the Congo and the Nile, they  
206 regulate timing and magnitude of runoff<sup>9</sup>. They also regulate local temperatures<sup>41</sup> and provide  
207 numerous other services to people in the surrounding landscapes<sup>9</sup>. Clearly, more should be done to  
208 avoid the destruction of these important ecosystems. Logging, mining and clearing land for farming,  
209 but also political unrest and militia presence have affected -and continue to affect- these forests, e.g.  
210 in Itombwe Mts in the Democratic Republic of the Congo<sup>42</sup>. Protected areas are known to help  
211 reduce deforestation in the tropics<sup>43</sup>. Beyond protected areas, other forest conservation  
212 mechanisms could be implemented, including effective carbon finance. Previous IPCC AGC-stock  
213 estimates for montane forests in Africa (89.3 Mg C ha<sup>-1</sup>) may have contributed to low incentives for  
214 carbon finance mechanisms in these ecosystems. Our study shows the far greater carbon storage  
215 potential in these tropical montane forests, which will be even higher if soil carbon stocks are  
216 considered (e.g. > 200 Mg C ha<sup>-1</sup> of organic carbon occurs in the top 0-30 cm soil on Mt Cameroon<sup>44</sup>  
217 and in the Usambara Mts, Tanzania<sup>45</sup>).

218  
219 As well as conserving the remaining montane forests, efforts to restore them are critical. Forest  
220 restoration at one of our sites, Kibale National Park in Uganda, indicates the potential for rapid AGC  
221 accumulation<sup>46</sup>. Our study shows the high potential AGC-stock these montane forests can attain. The  
222 possible co-benefits of forest restoration, notably water regulation, control of soil erosion and  
223 landslides and biodiversity conservation should also be considered. Most African nations are  
224 committed to the Bonn Challenge; Ethiopia leading with 15 million ha committed (Table 1). We  
225 provide country-specific estimates of potential AGC-stocks based on forests sampled in the AfriMont  
226 dataset to help guide such interventions (Table 1, Extended Data Fig. 10). Caution is needed when  
227 scaling-up our estimates to the landscape scale, as not all forests are closed-canopy old-growth and  
228 structurally intact. Remote sensing or ancillary data (landcover maps, spatial environmental data)  
229 could be used to identify e.g. exotic plantations, degraded or bamboo forests, and thus help create  
230 detailed AGC maps at different spatial scales<sup>18,47</sup>. A closer collaboration between air-borne, space-  
231 borne and ground approaches (such as the AfriMont and AfriTRON plot networks) is key for accurate  
232 quantification and monitoring of landscape-scale tropical forest AGC-stocks, particularly in mountain  
233 regions.

234  
235 Our newly compiled dataset and analysis provides a large-scale quantification of AGC-stock in  
236 African tropical montane forests, indicating it to be on average substantially higher than previously  
237 thought. While there is variation around this mean AGC-stock within and across sites, it is not  
238 systematically related to elevation. Apart from helping refine country-level estimates, IPCC  
239 guidelines and ground-calibration of remote-sensing estimates, continued on-the-ground monitoring  
240 of the AfriMont plot network will help determine ecosystem dynamics and carbon residence time in  
241 these extraordinarily carbon-rich forests, as well as their responses to climatic changes.

242  
243

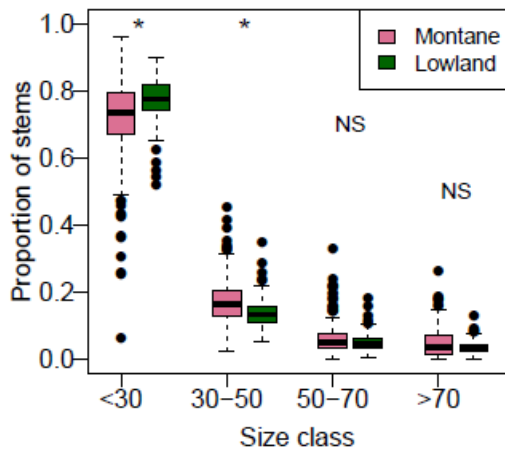
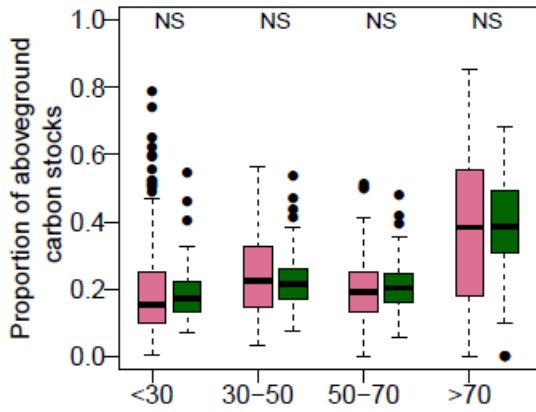


245  
246

247 **Fig. 1 | Pantropical variation in aboveground carbon stocks sampled by plot networks in montane**  
 248 **(≥ 800 m asl) and lowland (< 800 m asl) tropical forests.** Data from this study for African montane  
 249 forests ( $n = 226$  plots, this study), montane forests in the Neotropics ( $n = 131$ ) and Southeast Asia ( $n$   
 250  $= 32$ ) are from ref.<sup>2,5,6</sup>, lowland forests in Africa ( $n = 290$ ), the Neotropics ( $n = 416$ ) and Southeast  
 251 Asia ( $n = 60$ ) are from ref.<sup>7</sup>. Coloured points show the AGC-stock in each plot, with point size  
 252 proportional to square-root plot area. Black points show means for each continent-elevation  
 253 category estimated using linear mixed-effects models with site as a random effect, and lines show  
 254 95% confidence intervals around means. Letters indicate significant differences between continent  
 255 elevation category combinations (linear mixed-effects models with site as a random effect,  $P < 0.05$ ).

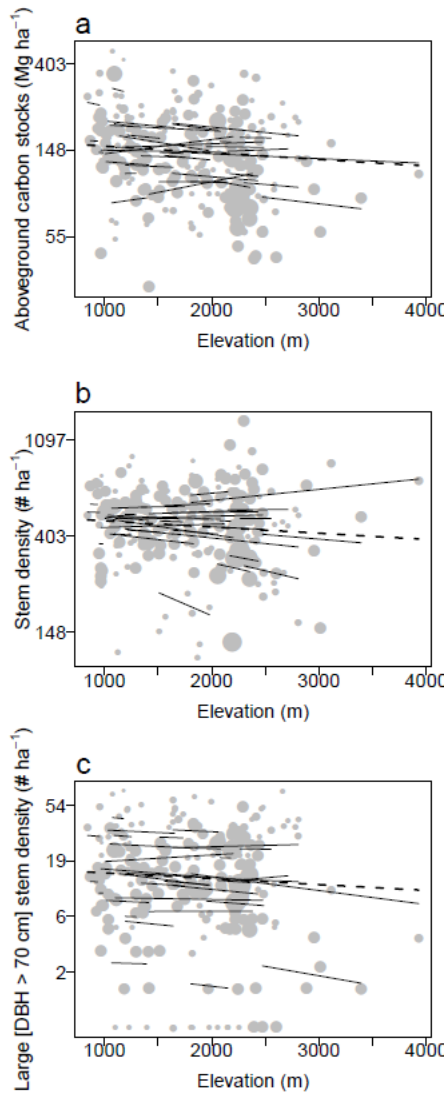
256  
257





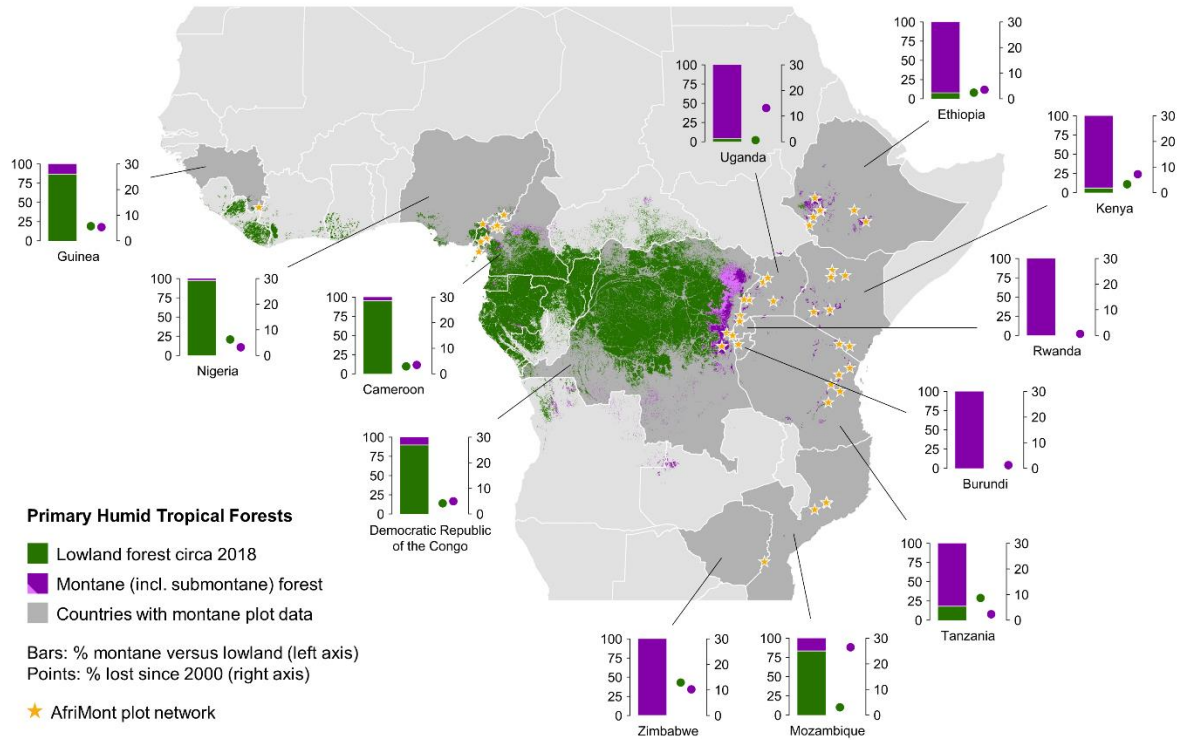
258  
 259  
 260  
 261  
 262  
 263  
 264  
 265  
 266

**Fig. 2 | Proportion of plot-level aboveground carbon stock and stems accounted for by each size class in montane and in lowland forests in Africa.** Statistically significant differences in contribution of each size class between montane and lowland forest plot networks are shown by asterisks (linear mixed-effects model,  $P < 0.05$ ). NS = non-significant difference. Montane ( $n = 226$ ), lowland ( $n = 132$ ). The thick line shows the median, and boxes cover the interquartile range (IQR). Values  $> 1.5$  times IQR away from the IQR are shown by points.



267  
 268  
 269  
 270  
 271  
 272  
 273  
 274  
 275  
 276  
 277  
 278  
 279

**Fig. 3 | Variables as a function of elevation.** a-c Relationship between elevation and plot-level AGC stock (a), stem density (b) and stem density of large stems (>70 cm diameter; c) for the AfriMont dataset. Note log-scale of y-axis. Each response variable was log-transformed and modelled as a function of elevation with a linear mixed-effect models with random slopes. The dashed line shows the relationship across sites (non-significant in all cases,  $P \geq 0.3$ , Table S4), while the black lines show the relationship within each site. Point sizes are proportional to square-root plot area. A polynomial model allowing a non-linear relationship with elevation was also tested but not supported over the linear model in any case ( $P \geq 0.7$ , Table S4). The absence of a significant relationship with elevation is robust to removing the two highest elevation sites, Rwenzori and Virunga (Table S4). DBH diameter at breast height.



280  
 281  
 282  
 283  
 284  
 285  
 286  
 287

**Fig. 4. | Old-growth evergreen humid forests in lowland and montane tropical Africa.** Forest extends circa 2018. Note that montane includes submontane forests (800-1,000 m asl, light purple). Montane forests represent most (or all) evergreen humid old-growth forest in ten African nations: Burundi, Ethiopia, Kenya, Rwanda, Tanzania, Uganda and Zimbabwe (included in AfriMont); and Zambia, Malawi and South Sudan (no plot data available). Forest cover extracted from ref.<sup>38</sup> and clipped to 'primary humid forest' using ref.<sup>39</sup>. See Table 1 for country-level absolute estimates.

288 **Table 1 | Remaining forest area and aboveground carbon estimates for montane and lowland**  
 289 **tropical forests in Africa**  
 290

Country	Montane (ha)	Montane lost (ha)	Montane AGC (MgC ha <sup>-1</sup> , 95% CI)	Montane sites (plots)	Lowland (ha)	Lowland AGC (MgC ha <sup>-1</sup> , 95% CI)	Lowland plots	Bonn Challenge by 2020 (ha)
Burundi	25,000	300	<b>94</b> (47-176)	1 (7)	0		0	2 million
Cameroon	840,000	30,200	<b>153</b> (121-195)	7 (37)	17.7 million	<b>166</b> (151-185)	72	12 million
DRC	10.2 million	536,500	<b>129</b> (84-202)	2 (37)	90 million	<b>158</b> (135-183)	48	8 million
Ethiopia	1.7 million	62,100	<b>165</b> (124-215)	8 (25)	145,000	<sup>a</sup>	0	15 million
Guinea	29,000	1,700	<b>314</b> (147-616) <sup>b</sup>	1 (2)	193,000	<b>157</b> (122 – 206) <sup>c</sup>	24	2 million
Kenya	568,000	44,100	<b>104</b> (79-136)	8 (38)	37,000		0	5.1 million
Mozambique	18,000	6,600 <sup>d</sup>	<b>226</b> (146-384) <sup>b</sup>	3 (4)	93,000	<sup>e</sup>	0	1 million
Nigeria	42,000	1,400	<b>120</b> (47-309) <sup>b</sup>	1 (1)	1.8 million	<b>161</b> (105-262)	2	4 million
Rwanda	53,000	300	<b>106</b> (65-168)	2 (11)	0		0	2 million
Tanzania	587,000	13,900	<b>175</b> (129-234)	6 (29)	130,000	<b>128</b> (101-163)	16	5.2 million
Uganda	427,000	64,600 <sup>d</sup>	<b>158</b> (111-209)	6 (23)	18,000		0	2.5 million
Zimbabwe	7,000	800 <sup>d</sup>	<b>203</b> (108-363)	1 (12)	<1,000		0	2 million

291

292 Forest cover circa 2018 was extracted from ref.<sup>38</sup> and clipped to 'primary humid forest' using ref.<sup>39</sup>.

293 Montane forest lost covers the period 2000-2018. Mean aboveground carbon (AGC, in MgC ha<sup>-1</sup>)

294 estimates for montane (or lowland) forests were estimated from AfriMont and AfriTRON plot

295 network data. Mean AGC values are in boldface, 95% confidence intervals in parentheses. For details

296 on sites and plots used see Table S5. Bonn Challenge pledges for 2030 not yet available.

297 <sup>a</sup> Ref.<sup>48</sup> report 192 MgC ha<sup>-1</sup> for lowland.

298 <sup>b</sup> Few plots sampled, or very small plots sampled, AGC estimates may not be robust, see Extended  
 299 data Fig. 10.

300 <sup>c</sup> Data from neighbouring Liberia.

301 <sup>d</sup>Montane forest loss in Mozambique, Uganda and Zimbabwe represents 27%, 13% and 10% of the  
 302 existing montane forest in 2001, respectively. Montane forest loss in Côte d'Ivoire (no plot data  
 303 available) was estimated to be 21% for the same period.

304 <sup>e</sup> Ref.<sup>49</sup> report 132.2 MgC ha<sup>-1</sup> for lowland.

305

306

307 **References**

- 308 1. Erb, K., et al. Unexpectedly large impact of forest management and grazing on global  
 309 vegetation biomass. *Nature* **553**, 73–76 (2018).
- 310 2. Spracklen, D.V. & Righelato, R. Tropical montane forests are a larger than expected global  
 311 carbon store. *Biogeosciences* **11**, 2741–2754 (2014).
- 312 3. Fahey, T. J., Sherman, R. E. & Tanne, E. V. J. Tropical montane cloud forest: environmental  
 313 drivers of vegetation structure and ecosystem function. *J. Trop. Ecol.* **32**, 355–367 (2016).
- 314 4. Lewis, S. L. et al. Above-ground biomass and structure of 260 African tropical forests. *Phil.*  
 315 *Trans. R. Soc. Lond. B* **368**, 20120295 (2013).
- 316 5. Vilanova, E. et al. Environmental drivers of forest structure and stem turnover across  
 317 Venezuelan tropical forests. *PLoS ONE* **13**(6): e0198489 (2018).
- 318 6. Alvarez-Davila, E. et al. Forest biomass density across large climate gradients in northern  
 319 South America is related to water availability but not with temperature. *PLoS ONE* **12**(3):  
 320 e0171072 (2017).
- 321 7. Sullivan, M. J. P., et al. Long-term thermal sensitivity of Earth’s tropical forests. *Science* **368**,  
 322 869–874 (2020).
- 323 8. Domke, G. et al. in 2019 Refinement to the 2006 IPCC Guidelines for National Greenhouse  
 324 Gas Inventories Vol. 4 (eds Calvo Buendia, E. et al.) Ch. 4, 48 (IPCC, 2019).
- 325 9. *African Mountains Atlas* (UNEP, 2014).
- 326 10. Rahbek, C., et al. Humboldt’s enigma: What causes global patterns of mountain biodiversity?  
 327 *Science* **365**, 1108–1113 (2019).
- 328 11. Pan, Y. et al. A large and persistent carbon sink in the world’s forests. *Science* **333**, 988–993  
 329 (2011).
- 330 12. Booth, B. B. B. et al. High sensitivity of future global warming to land carbon cycle processes.  
 331 *Environ. Res. Lett.* **7**, 024002 (2012).
- 332 13. Hubau, W., et al. Asynchronous carbon sink saturation in African and Amazonian tropical  
 333 forests. *Nature* **579**, 80–87 (2020).
- 334 14. Feldpausch, T. R. et al. Tree height integrated into pantropical forest biomass estimates.  
 335 *Biogeosciences* **9**, 3381–3403 (2012).
- 336 15. Bastin, J.-F., et al. Pan-tropical prediction of forest structure from the largest trees. *Global*  
 337 *Ecol. Biogeogr.* **27**, 1366–1383 (2018).
- 338 16. CCI BIOMASS Product User Guide Year 1 Version 1.0. (Aberystwyth University and GAMMA  
 339 Remote Sensing, 2019)  
 340 [https://climate.esa.int/sites/default/files/biomass\\_D4.3\\_Product\\_User\\_Guide\\_V1.0.pdf](https://climate.esa.int/sites/default/files/biomass_D4.3_Product_User_Guide_V1.0.pdf)
- 341 17. Lefsky, M. A., Keller, M., Pang, Y., de Camargo, P. & Hunter, M. O. Revised method for forest  
 342 canopy height estimation from the Geoscience Laser Altimeter System waveforms. *J. Appl.*  
 343 *Remote Sens.* **1**, 013537 (2007).
- 344 18. Willcock, S., et al. Quantifying and understanding carbon storage and sequestration within  
 345 the Eastern Arc Mountains of Tanzania, a tropical biodiversity hotspot. *Carbon Balance*  
 346 *Manage.* **9**, 2 (2014).
- 347 19. Bussmann, R.W. Vegetation zonation and nomenclature of African Mountains – An  
 348 overview. *Lyonia* **11**, 41–66 (2006).
- 349 20. Hamilton, A. Vegetation, climate and soil, altitudinal relationships on the East Usambara  
 350 Mountains of Tanzania. *J. E. Afr. Nat. Hist.* **87**, 1-5 (1998).
- 351 21. Phillips, O., Baker, T., Brienen, R. & Feldpausch, T. RAINFOR field manual for plot  
 352 establishment and remeasurement.  
 353 [http://www.rainfor.org/upload/ManualsEnglish/RAINFOR\\_field\\_manual\\_version\\_2016.pdf](http://www.rainfor.org/upload/ManualsEnglish/RAINFOR_field_manual_version_2016.pdf)  
 354 (Univ. Leeds, 2016).
- 355 22. Jarvis, A. & Mulligan, M., The climate of cloud forests. *Hydrol. Process.* **25**, 327–343 (2011).
- 356 23. Platts, P.J., Omeny, P.A. & Marchant, R. AFRICLIM: high-resolution climate projections for  
 357 ecological applications in Africa. *Afr. J. Ecol.* **53**, 103–108 (2015).

- 358 24. McInerney, G. J., Purves, D. W. Fine-scale environmental variation in species distribution  
359 modelling: Regression dilution, latent variables and neighbourly advice. *Methods Ecol. Evol.*  
360 **2**, 248–257 (2011).
- 361 25. Poulsen, J.R., et al. Ecological consequences of forest elephant declines for Afrotropical  
362 forests. *Conserv. Biol.* **32**, 559–567 (2018).
- 363 26. Berzaghi, F., et al. Carbon stocks in central African forests enhanced by elephant  
364 disturbance. *Nat. Geosci.* **12**, 725–729 (2019).
- 365 27. Enquist, B.J., et al. The megabiota are disproportionately important for biosphere  
366 functioning. *Nat. Commun.* **11**, 699 (2020).
- 367 28. Lin, T.-C., Hogan, J.A. & Chang, C.T. Tropical Cyclone Ecology: A Scale-Link Perspective.  
368 *Trends Ecol. Evol.* **35**, 594–604 (2020).
- 369 29. Favalli, M., et al. Lava flow hazard and risk at Mt. Cameroon volcano. *Bull. Volcanol.* **74**, 423–  
370 439 (2012).
- 371 30. Stanley, T. & Kirschbaum, D.B. A heuristic approach to global landslide susceptibility  
372 mapping. *Nat. Hazards* **87**, 145–164 (2017).
- 373 31. Lovett, J. C. Elevational and latitudinal changes in tree associations and diversity in the  
374 Eastern Arc mountains of Tanzania. *J. Trop. Ecol.* **12**, 629–650 (1996).
- 375 32. Hemp, A., et al. Africa’s highest mountain harbours Africa’s tallest trees. *Biodiv. Conserv.* **26**,  
376 103–113 (2016).
- 377 33. Culmsee, H., Leuschner, C., Moser, G. & Pitopang, R., Forest aboveground biomass along an  
378 elevational transect in Sulawesi, Indonesia, and the role of Fagaceae in tropical montane rain  
379 forests. *J. Biogeogr.* **37**, 960–974 (2010).
- 380 34. Enright, N.J. & Ogden, J. The southern conifers - a synthesis. Ecology of the southern conifers  
381 (ed. by N.J. Enright & Hill R.S.), pp. 271–287. Melbourne University Press, Melbourne (1995).
- 382 35. Neale, D. B. & Wheeler, N. C. The Conifers. In: The Conifers: Genomes, Variation and  
383 Evolution (eds. Neale, D. B. & Wheeler, N. C.) pp 1–21. Springer International Publishing  
384 (2019).
- 385 36. Mill, R. R. Towards a Biogeography of the Podocarpaceae. In IV International Conifer  
386 Conference, R. R. Mill, ed. *Acta Hort.* **615**, 137–147 (2003).
- 387 37. Helmer, E.H., Gerson, E.A., Baggett, L.S., Bird, B.J., Ruzycski, T.S. & Voggeser, S.M.  
388 Neotropical cloud forests and paramo to contract and dry from declines in cloud immersion  
389 and frost. *PLoS ONE* **14**(4): e0213155 (2019).
- 390 38. Hansen, M. C., et al. High-Resolution Global Maps of 21st-Century Forest Cover Change.  
391 *Science* **342**, 850-853 (2013).
- 392 39. Turubanova, S., Potapov, P., Tyukavina, A. & Hansen M. Ongoing primary forest loss in Brazil,  
393 Democratic Republic of the Congo, and Indonesia. *Environ. Res. Lett.* **13**, 074028 (2018).
- 394 40. Pellikka, P. K. E., Lötjönen, M., Siljander, M. & Lens, L. Airborne remote sensing of  
395 spatiotemporal change (1955–2004) in indigenous and exotic forest cover in the Taita Hills,  
396 Kenya. *Int. J. Appl. Earth Obs.* **11**, 221–232 (2009).
- 397 41. Zeng, Z. et al. Deforestation-induced warming over tropical mountain regions regulated by  
398 elevation. *Nat. Geosci.* **14**, 23–29 (2020). <https://doi.org/10.1038/s41561-020-00666-0>
- 399 42. Spira, C., Kirkby, A., Kujirakwinja, D. & Plumptre, A. J. The socio-economics of artisanal  
400 mining and bushmeat hunting around protected areas: Kahuzi– Biega National Park and  
401 Itombwe nature reserve, eastern Democratic Republic of Congo. *Oryx* **53**, 136–144(2017).
- 402 43. Bebbler, D.P. & Butt, N. Tropical protected areas reduced deforestation carbon emissions by  
403 one third from 2000-2012. *Sci. Rep.* **7**, 14005 (2017).
- 404 44. Tegha, K. C. & Sendze, Y. G., Soil organic carbon stocks in Mt Cameroon National Park under  
405 different land uses. *J. Ecol. Nat. Environ.* **8**, 20–30, (2016).
- 406 45. Munishi, P.K.T. & Shear, T.H. Carbon storage in afro-montane rain forests of the eastern arc  
407 mountains of Tanzania: their net contribution to atmospheric carbon. *J. Trop. For. Sci.* **16**,  
408 78–98 (2004).

- 409 46. Wheeler, C.E., et al. Carbon sequestration and biodiversity following 18 years of active  
410 tropical forest restoration. *Forest Ecol. Manage.* **373**, 44–55 (2016).
- 411 47. Avitabile, V., Baccini, A., Friedl, M.A. & Schimullius, C. Capabilities and limitations of Landsat  
412 and land cover data for aboveground woody biomass estimation of Uganda. *Remote Sens.*  
413 *Environ.* **117**, 366–380 (2012).
- 414 48. Aneseyee, B A., Soromessa, T. & Belliethathan, S. Carbon Sock of Gambella National Park:  
415 Implication for Climate Change Mitigation. *Int. J. Adv. Life Sci.* **35**, 41–56 (2015).
- 416 49. Lisboa, S.N., et al. Biomass allometric equation and expansion factor for a mountain moist  
417 evergreen forest in Mozambique. *Carbon Balance Manage.* **13**, 23 (2018).

418

## 419 **Methods**

### 420 **AfriMont or montane Africa dataset**

421 We compiled forest inventory plot data from the African Tropical Rainforest Observatory Network  
422 (AfriTRON; [www.afritron.org](http://www.afritron.org)), with data curated at [www.ForestPlots.net](http://www.ForestPlots.net)<sup>50,51</sup> and the TEAM  
423 network<sup>52</sup>, as well as from numerous site-specific publications detailed in Table S5 and mapped in  
424 Fig. 4. Plots were selected for the analysis when conforming to the following criteria: ≥800 m asl,  
425 closed-canopy evergreen wet or moist tropical forest, geo-referenced, old-growth and structurally  
426 intact (not impacted by recent selective logging, fire or coffee cultivation), with no exotic species  
427 present (e.g. *Eucalyptus* or *Pinus* spp.), all trees ≥10 cm diameter measured and majority of stems  
428 identified to species. We included plots from Virunga Massif in Rwanda/Uganda even when not  
429 100% closed-canopy due to high abundance of naturally-occurring bamboo. In all plots, tree  
430 diameter was measured at 1.3 m along the stem from the ground, or above buttresses if present. In  
431 23 sites tree height was sampled in the field for some stems, using a clinometer or a laser. Families  
432 and species names follow the African Plant Database (<http://africanplantdatabase.ch>). The AfriMont  
433 dataset consists of 72,336 stems, of which 92.9% were identified to species, 98.4% to genus and  
434 98.5% to family. This dataset represents a standardised safe long-term repository of valuable  
435 historical data (four sites initially considered could not be included because tree-level data had  
436 already been lost by data owners).

437

### 438 **AfriTRON or lowland Africa dataset**

439 The 132 lowland-forest plots are all from AfriTRON<sup>4,13,53</sup>. They were selected using the same criteria  
440 as above (but with elevation <800 m asl), restricted to countries for which we also had montane  
441 plots plus neighbouring countries where the mountains span international borders (e.g. Mt Nimba  
442 spans Guinea and Liberia). The dataset includes 51,305 stems, of which 89.6% were identified to  
443 species, 97.3% to genus and 97.7 % to family. The plot data were retrieved from forestplot.net on  
444 06/01/2019. The plot locations and details are in Table S6.

445

### 446 **Literature dataset**

447 We compiled data on AGC-stocks in tropical lowland and montane forests to compare to the  
448 AfriMont data. Data for lowland forests came from ref.<sup>7</sup> and consisted of all multi- and single-census  
449 plots that were <800 m asl. Data for montane forests were obtained from ref.<sup>2</sup>, with additional data  
450 from Venezuela (ref.<sup>5</sup>) and Colombia (ref.<sup>6</sup>). Montane plots were defined as ≥800 m asl; elevation  
451 was not provided for the Colombian dataset so plots were selected based on the forest type, and  
452 these plots were excluded from analyses requiring elevation. To avoid double counting plots,  
453 Venezuelan and Colombian plots were removed from the ref.<sup>2</sup> dataset.

454

### 455 **Aboveground carbon**

456 For each tree in the montane dataset we used the published allometric equation by ref.<sup>54</sup> to  
457 estimate aboveground biomass. This allometric equation was created using data from directly  
458 harvested trees at 58 sites across the tropics, including eight sites with elevation ≥800m asl (range  
459 900-3,000m asl including sites in Africa). We then converted this biomass to carbon, assuming that

460 aboveground carbon (AGC, in  $\text{Mg C ha}^{-1}$ ) is 45.6% of aboveground biomass<sup>55</sup>. AGC for each plot was  
461 estimated as the sum of the AGC of each living stem, divided by planimetric plot area (in hectares). If  
462 field measurements of slope were unavailable, we converted surface to planimetric area extracting  
463 slope from the NASA's Shuttle Radar Topography Mission (SRTM) product. We excluded tree ferns,  
464 bamboo and palms, as these were not measured in all plots. Ref.<sup>54</sup> includes tree diameter, wood  
465 mass density and tree height. The best taxonomic match wood density of each stem was extracted  
466 from a global database<sup>56,57</sup> following ref.<sup>53</sup>. For some sites, all trees in a plot had been sampled for  
467 height. If this was not the case, but some field measurements of height were available (typically ten  
468 stems per diameter class), we constructed a site-specific height-diameter model, using a Weibull  
469 equation following ref.<sup>58</sup>. If no field measurements of height were available, we constructed a  
470 cluster-specific height-diameter model, using a Weibull equation, as explained in Table S7 in  
471 Supplementary Information. The same approach was used to calculate aboveground biomass for  
472 lowland forests. For these, height was estimated using a Weibull equation following ref.<sup>58</sup>.

473

#### 474 **Small plots and data subsampling**

475 For 22 sites where plots were small ( $<0.2$  ha), we aggregated plots to groups of about 0.2 ha based  
476 on their geographic proximity, elevation, environmental affinity and the co-authors' knowledge of  
477 the site, to help reduce the variation among plots at site level. This is because the presence of an  
478 extremely large tree in a small plot can result in overestimates of AGC<sup>59</sup>. We investigated if using the  
479 aggregated-plot approach affected AGC-stock estimates at the site level, and this was not the case  
480 (Extended Data Fig. 2). We also investigated if including small plots affected the continental mean  
481 AGC-stock estimates, as small plots have greater edge surface, and there is a tendency of some field  
482 teams to include large trees inside plots when laying out the boundaries<sup>60</sup>. Including small plots did  
483 not significantly affect our continental mean AGC-stock estimates (Extended Data Fig. 2). We also  
484 explored the sensitivity of our continental mean AGC-stock estimates to data subsampling. Data  
485 were resampled at different sample sizes either at plot level (sampling with replacement) or at site  
486 level (sampling without replacement). The number of plots ( $n=226$ ) and the number of sites ( $n=44$ )  
487 we sampled indicate that our estimates of AGC-stock at the continental level are robust (Extended  
488 Data Fig. 1). They are also not affected by the fact that we included plots 800-1,000 m asl (Extended  
489 Data Fig. 3).

490

#### 491 **Size classes**

492 For all plots, we computed the proportion of AGC which was distributed in each size-diameter class,  
493 using the classes of ref.<sup>15</sup>. We also computed stem density, basal area, density of large trees ( $>70$  cm  
494 diameter, named  $SD_{70}$  in stems  $\text{ha}^{-1}$ ) and Podocarpaceae abundance (in percentage of plot-level  
495 basal area).

496

#### 497 **Environmental variables and their effects**

498 Climate variables (temperature annual mean and seasonality, and precipitation mean and  
499 seasonality, i.e. Bio1, 4, 12 and 15) were extracted from WorldClimV2<sup>61</sup> at 30 arc-sec ( $\sim 1$ -km)  
500 resolution. Mean temperature values were adjusted for the difference in elevation between the plot  
501 and the wider 1-km grid cell using the lapse rate of  $-0.005^\circ\text{C m}^{-1}$ . We obtained data on cloud cover  
502 from ref.<sup>62</sup> and lightning frequency (0.1 degree,  $\sim 11$  km) from the Lightning Imaging Sensor (LIS) very  
503 high resolution climatology<sup>63</sup>. Values for soil variables (cation exchange capacity, CEC, representing  
504 soil fertility, and percentage clay representing soil texture) were extracted from SoilGrids<sup>64</sup> ( $\sim 1$ -km  
505 resolution) and a depth-weighted mean taken for values from 0 to 30 cm depth to give a single value  
506 of each soil variable per plot. Elevation was obtained from SRTM (at 3 arc-second resolution,  $\sim 90$  m).  
507 Topographic metrics were calculated from elevation data using the terrain function in the raster R  
508 package version 3.3-6. These were slope and topographic position index (TPI). TPI is the difference  
509 between the elevation of the plot and the mean value of the eight surrounding grid cells – positive  
510 values indicate locally high locations and negative values indicate locally low locations. Where small



511 plots were aggregated for analysis, environmental variables were extracted for the ungrouped plot  
512 locations, and then an area-weighted mean taken to obtain a plot-level value.

513

#### 514 **Elephant and conifer effects on AGC-stocks**

515 For the current elephant presence in the AfriMont plots, we created a binary variable  
516 (presence/absence) based on co-authors knowledge of elephant ranges and elevation distribution at  
517 each site as of 2019. Co-authors estimated that elephants were present in 2019 in 54 plots in 12  
518 sites in five countries (see Table S5). For all plots which had at least one individual in the  
519 Podocarpaceae family (47 plots, 16 sites, 7 countries), we computed the contribution of  
520 Podocarpaceae to plot basal area and AGC-stock in terms of percentages.

521

#### 522 **Estimating forest cover and loss**

523 We obtained estimates of forest cover and loss in the years 2000 through to 2018, using the 'loss  
524 year' dataset of the Global Forest Change database, version 1.6 (ref.<sup>38</sup>). To exclude plantation  
525 forests, 'dry' forests (e.g. miombo woodland) and degraded forests, we applied the 'primary humid  
526 forest' mask developed by ref.<sup>39</sup>. We distinguished montane from lowland forests using an  
527 elevational cut-off of 800-m elevation, using the SRTM v3 product at 1 arc-sec resolution (snapping  
528 to the ref.<sup>38</sup> grid of the same resolution). Where there were gaps in the 1 arc-sec SRTM product, we  
529 filled these using a 1 arc-sec bilinear interpolation of the (gapless) 3 arc-sec SRTM product. Areal  
530 estimates of forest cover and loss were calculated at 30-m resolution using the Africa Sinusoidal  
531 projection. To estimate future forest loss by year 2030, we extrapolated absolute country-level  
532 deforestation rates for the period 2000-2018 (in ha per year).

533

#### 534 **Investigating AfriMont representativeness**

535 To quantify AfriMont sampling effort within the montane forest biome in Africa, we used the map of  
536 tropical montane forest extent (see above) and calculated the amount of remaining forest in each 1-  
537 degree grid-cell. By dividing the area sampled in the AfriMont dataset by the proportion of this  
538 biome in a grid-cell, we calculated the expected sampling intensity if sampling was proportional to  
539 remaining forest extent. To assess how representative our plot network was of the environmental  
540 conditions of the wider tropical montane forest biome in Africa, we extracted the environmental  
541 data (climate and soil variables presented above) at ~1-km resolution from grid-cells that contained  
542 montane forest. We then visually compared the distribution of each variable in our dataset to its  
543 distribution across the biome (Extended Data Fig. 7).

544

#### 545 **AfriMont vs global AGC maps**

546 We extracted alternative AGC estimates for the AfriMont plots (unaggregated, n=666) from four  
547 different sources: Harris et al. (ref.<sup>65</sup>) (30-m resolution, dated 2000), the European Space Agency  
548 Climate Change Initiative Biomass map<sup>66</sup> (100-m resolution, 2017), Saatchi, et al. (ref.<sup>67</sup>) (1-km  
549 resolution, 2007/8) and Avitabile et al. (ref.<sup>68</sup>) (1-km resolution, circa 2000-2010). Most of the  
550 AfriMont plots were sampled between 2000 and 2019 (Table S5). Where the plots were found within  
551 a single map pixel, we extracted that value. Where plots were larger than the pixel size, we averaged  
552 the values from the surrounding pixels weighted according to the proportion of the pixel that was in  
553 the plot.

554

#### 555 **Statistical analysis**

556 Data were analysed using linear mixed-effects models, with site as a random effect. Site was  
557 included as a random intercept in all models, and as a random slope where relationships were  
558 assessed against elevation. Allowing the slope of the elevation effect to vary amongst sites in this  
559 way captures the *a priori* expectation for slopes to differ among sites, for example due to mass  
560 elevation effects. The effect of plot size on variation was accounted for by weighting observations by  
561 a power transformation of plot size; this was estimated during model fitting using the varPower

562 function in the nlme R package (ref.<sup>69</sup>), and then models refitted using the lme4 R package (ref.<sup>70</sup>)  
563 using these estimated weights. Confidence intervals and *P*-values for mixed effects models  
564 parameters were estimated by bootstrapping models (1,000 iterations) using the  
565 bootstrap\_parameters function in the parameters R package (ref.<sup>71</sup>). AGC-stocks, stem density and  
566 SD<sub>70</sub> were natural-log transformed (a small constant was added to SD<sub>70</sub> before log transforming to  
567 avoid log-transforming zeros) to meet assumptions of normality and avoid heteroscedacity. Likewise,  
568 the proportional contribution of each size class was square-root transformed. Differences in AGC-  
569 stocks between all combinations of lowland and montane forests amongst continents were assessed  
570 using Tukey post-hoc tests implemented in the multcomp R package (ref.<sup>72</sup>). Relationships between  
571 AGC-stocks and environmental variables were investigated by fitting all subsets of the full model  
572 with all environmental covariates and averaging the best supported (difference in Akaike  
573 information criterion from the best supported model  $\Delta\text{AIC} < 4$ ) models (using dredge and movel.avg  
574 functions in the MuMIn R package (ref.<sup>73</sup>). We used these relationships with climate and soil to  
575 predict AGC-stocks in each 1-km grid cell containing montane forests (holding topographic variables  
576 at their dataset wide mean), and then took the forest-area weighted mean of these to obtain a  
577 single mean for the tropical montane forest biome in Africa. Differences in AGC-stocks between  
578 plots with and without elephants were tested using t-test with AGC-stocks natural-log transformed.  
579 We investigated if Podocarpaceae abundance (in terms of basal area) and plot AGC-stocks were  
580 significantly correlated using Spearman's rank correlation coefficient. To investigate if sampling  
581 design affected AfriMont AGC-stock estimates we used ANOVA to test whether site-level mean AGC-  
582 stocks differed according to the sampling strategy used to establish plots at that site. To explore the  
583 relationship between AfriMont AGC-stock estimates and global maps, and among these global maps,  
584 we used Spearman's rank correlation test.

585

## 586 **References Methods**

- 587 50. Lopez-Gonzalez, G., Lewis, S. L., Burkitt, M. & Phillips, O. L. ForestPlots.net: a web application  
588 and research tool to manage and analyse tropical forest plot data. *J. Veg. Sci.* **22**, 610–613  
589 (2011).
- 590 51. Lopez-Gonzalez, G., Lewis, S. L., Burkitt, M., Baker, T. R. & Phillips, O. L. ForestPlots.net  
591 Database <http://www.forestplots.net> (2009).
- 592 52. Cavanaugh, K., et al. Carbon storage in tropical forests correlates with taxonomic diversity  
593 and functional dominance on a global scale. *Global Ecol. Biogeogr.* **23**, 563–573 (2014).
- 594 53. Lewis, S. L., et al. 2009 Increasing carbon storage in intact African tropical forests. *Nature*  
595 **457**, 1003–1006 (2009).
- 596 54. Chave, J. et al. Improved allometric models to estimate the aboveground biomass of tropical  
597 trees. *Glob. Change Biol.* **20**, 3177–3190 (2014).
- 598 55. Martin, A. R., Doraisami, M. & Thomas, S. C. Global patterns in wood carbon concentration  
599 across the world's trees and forests. *Nat. Geosci.* **11**, 915–920 (2018).
- 600 56. Chave, J. et al. Towards a worldwide wood economics spectrum. *Ecol. Lett.* **12**, 351–366  
601 (2009).
- 602 57. Zanne, A. E. et al. Towards a Worldwide Wood Economics Spectrum  
603 <https://doi.org/10.5061/dryad.234> (Dryad Digital Repository, 2009).
- 604 58. Clark, D.A., Brown, S., Kicklighter, D.W., Chambers, J.Q., Thomlinson, J.R., Ni, J. & Holland,  
605 E.A. Net primary production in tropical forests: an evaluation and synthesis of existing field  
606 data. *Ecol. Appl.* **11**, 371–384 (2001).
- 607 59. Paul, T.S.H., Kimberley, M.O. & Beets, P.N. Thinking outside the square: Evidence that plot  
608 shape and layout in forest inventories can bias estimates of stand metrics. *Methods Ecol.*  
609 *Evol.* **10**, 381–388 (2019).
- 610 60. Fick, S.E. & Hijmans, R.J., WorldClim 2: new 1-km spatial resolution climate surfaces for  
611 global land areas. *Int. J. Climatol.* **37**, 4302–4315 (2017).

- 612 61. Wilson, A.M. & Jetz, W. Remotely sensed high-resolution Global Cloud Dynamics for  
613 predicting ecosystem and biodiversity distributions. *PLoS Biol* **14**(3): e1002415 (2016).
- 614 62. Albrecht, R., Goodman, S., Buechler, D., Blakeslee R. & Christian, H. LIS 0.1 Degree Very High  
615 Resolution Gridded Lightning Climatology Data Collection. Data sets available online  
616 [<https://ghrc.nsstc.nasa.gov/pub/lis/climatology/LIS/>] from the NASA Global Hydrology  
617 Resource Center DAAC, Huntsville, Alabama, U.S.A. doi:  
618 <http://dx.doi.org/10.5067/LIS/LIS/DATA306>
- 619 63. Hengl, T., et al. SoilGrids250m: Global gridded soil information based on machine learning.  
620 *PLoS ONE* **12**(2): e0169748 (2017).
- 621 64. Harris, N. L. et al. Global maps of twenty-first century forest carbon fluxes. *Nat. Clim. Change*  
622 **11**, 234–240 (2021).
- 623 65. Santoro, M. & Cartus, O. ESA Biomass Climate Change Initiative (Biomass\_cci): Global  
624 datasets of forest above-ground biomass for the year 2017, v1. Centre for Environmental  
625 Data Analysis, 2019. doi:10.5285/bedc59f37c9545c981a839eb552e4084
- 626 66. Saatchi, S., et al. Benchmark map of forest carbon stocks in tropical regions across three  
627 continents. *PNAS* **108**, 9899–9904 (2011).
- 628 67. Avitabile, V., et al. An integrated pan-tropical biomass map using multiple reference  
629 datasets. *Glob. Change Biol.* **22**, 1406–1420 (2016).
- 630 68. Pinheiro, J., Bates, D., DebRoy, S., Sarkar, D. & R Core Team. nlme: Linear and Nonlinear  
631 Mixed Effects Models. R package version 3.1-151, <https://CRAN> (2020).
- 632 69. Bates, D. Maechler, M., Bolker B. & Walker, S. Fitting Linear Mixed-Effects Models Using  
633 lme4. *J. Stat. Softw.* **67**, 1–48 (2015).
- 634 70. Lüdtke, D., Ben-Shachar, M., Patil, I. & Makowski, D. Parameters: extracting, computing  
635 and exploring the parameters of statistical models using R. *J. Open Source Softw* **5**, 2445  
636 (2020).
- 637 71. Hothorn, T., Bretz, F. & Westfall, P. Simultaneous Inference in General Parametric Models.  
638 *Biometrical Journal* **50**, 346–363 (2008).
- 639 72. Barton, K. 2020. MuMIn: Multi-Model Inference. R package version 1.43.17.

640

## 641 **Acknowledgements**

642 We sincerely thank the people of the many villages and local communities who welcomed our field  
643 teams and became our field assistants, without whose support the AfriMont dataset would not have  
644 been possible. *Cameroon*: villages Elak-Oku, Bokwoango, Bakingili, Muandelengoh, Enyandong,  
645 Ekangmbeng, Ngalmoa, Dikome Balue, Muyange, Matamani; assistants: E. Ndivé, D. Wultof, F.  
646 Keming, E. Bafon, J. Meyeih, T. K. Konsum, J. Esembe, F. Luma, F. Teke, E.E. Dagobert, E.D. Ndode,  
647 N.F. Njikang; *DRC*: Bunyakiri, J. Kalume, W. Gului, D. Cirhagaga, B. Mugisho; *Kenya*: assistants: A.M.  
648 Aide, H. Lerapo, J. Harugura, R.A. Wamuro, J. Lekatap, L. Lemooli, D. Kimuzi, B.M. Lombo, J. Broas, J.  
649 Hietanen, V. Heikinheimo, E. Schäfer; *Rwanda*: assistants: I. Rusizana, P. Niyontegereje, J.B. Gakima,  
650 F. Ngayabahiga; *Tanzania*: TEAM staff and affiliates; *Uganda*: K. Laughlin, X. Mugumya, L. Etwodu, M.  
651 Mugisa.

652

653 For logistical and administrative support, we are indebted to international, national and local  
654 institutions: SOPISDEW, Mt Cameroon National Park, Tropical Plant Exploration Group (TroPEG),  
655 Institut Congolais de Conservation de la Nature, Kahuzi-Biega National Park, Itombwe Nature  
656 Reserve, NEMA Marsabit Office, Taita Research Station, Kenya Forest Service, Rwanda Development  
657 Board, Nyungwe National Park, Conservation International, the Smithsonian Institution, Wildlife  
658 Conservation Society, Sokoine University of Agriculture, Tanzania Wildlife Research  
659 Institute, Tanzania National Parks Authority, Kilimanjaro National Park, Tanzania Commission for  
660 Science and Technology, Royal Zoological Society of Scotland, Uganda Wildlife Authority, Makerere  
661 University Biological Field Station, Uganda National Forestry Authority, Uganda National Council for  
662 Science and Technology.

663

664 Field campaigns for AfriMont were funded by Marie Skłodowska-Curie Actions Intra-European  
665 Fellowships (number 328075) and Global Fellowships (number 74356), National Geographic Explorer  
666 (NGS-53344R-18), Czech Science Foundation (no. 21-17125S), Rufford Small Grant Foundation  
667 (16712-B, 19476-D), Ministry of Foreign Affairs of Finland (BIODEV project), the Academy of Finland  
668 (number 318645), Swedish International Development Cooperation Agency, the Leverhulme Trust,  
669 the Strategic Research Area Biodiversity and Ecosystem Services in a Changing Climate, the German  
670 Research Foundation (DFG), Gatsby Plants, Natural Science and Engineering Research Council of  
671 Canada and International Development Research Centre of Canada.

672

673 This paper is also a product of the AfriTRON network, for which we are indebted to hundreds of  
674 institutions, field assistants and local communities for establishing and maintaining the plots,  
675 including: the Forestry Development Authority of the Government of Liberia, the University of  
676 Liberia, University of Ibadan (Nigeria), the University of Abeokuta (Nigeria), the University of  
677 Yaounde I (Cameroon), the National Herbarium of Yaounde (Cameroon), the University of Buea  
678 (Cameroon), Bioversity International (Cameroon), Salonga National Park (Democratic Republic of  
679 Congo), The Centre de Formation et de Recherche en Conservation Forestière (CEFRECOF, Epulu,  
680 Democratic Republic of Congo), the Institut National pour l'Étude et la Recherche Agronomiques  
681 (INERA, Democratic Republic of Congo), the École Régionale Postuniversitaire d'Aménagement et de  
682 Gestion intégrés des Forêts et Territoires tropicaux (ERAIFT Kinshasa, Democratic Republic of  
683 Congo), WWF-Democratic Republic of Congo, WCS-Democratic Republic of Congo, the Université de  
684 Kisangani (Democratic Republic of Congo), Université Officielle de Bukavu (Democratic Republic of  
685 Congo), Université de Mbuji-Mayi (Democratic Republic of Congo), le Ministère de l'Environnement et  
686 Développement Durable (Democratic Republic of Congo), the FORETS project in Yangambi (CIFOR,  
687 CGIAR and the European Union; Democratic Republic of Congo), the Lukuru Wildlife Research  
688 Foundation (Democratic Republic of Congo), Mbarara University of Science and Technology (MUST,  
689 Uganda), WCS-Uganda, the Uganda Forest Department, the Commission of Central African Forests  
690 (COMIFAC), the Udzungwa Ecological Monitoring Centre (Tanzania) and the Sokoine University of  
691 Agriculture (Tanzania). The AfriTRON network has been supported by the European Research  
692 Council (291585, 'T-FORCES' – Tropical Forests in the Changing Earth System, Advanced Grant to  
693 O.L.P. and S.L.L.), the Gordon and Betty Moore Foundation, the David and Lucile Packard  
694 Foundation, the European Union's Seventh Framework Programme (283080, 'GEOCARBON').

695

696 We are particularly grateful to A. Daniels, F. Mbayu, T.R. Feldpausch, E. Kearsley, J. Lloyd, R. Lowe, J.  
697 Mukinzi, L. Ojo, A.T. Peterson, J. Talbot and L. Zemagho for giving us access to their plot data. We  
698 also thank C. Chatelain (Geneva Botanic Gardens) for access to the African Plants Database and to H.  
699 Tang for helping explore the use of GEDI data.

700

701 Data from AfriTRON and most of AfriMont are stored and curated by ForestPlots.net, a long-term  
702 cyberinfrastructure initiative hosted at the University of Leeds that unites permanent plot records  
703 and their contributing scientists from the world's tropical forests. The development of  
704 ForestPlots.net and curation of African data have been funded by many sources, including the ERC  
705 (principally from AdG 291585 'T-FORCES'), the UK Natural Environment Research Council (including  
706 NE/B503384/1, NE/F005806/1, NE/P008755/1, NE/N012542/1 and NE/I028122/1), the Gordon and  
707 Betty Moore Foundation ('RAINFOR', 'MonANPeru'), the EU Horizon programme (especially  
708 'GEOCARBON', 'Amazalert') and the Royal Society (University Research Fellowship to S.L.L.).

709

#### 710 **Author Contributions**

711 A.C-S. conceived the study and assembled the AfriMont dataset. A.C-S. and M.J.P.S. analysed the  
712 plot data (with contributions from S.L.L.) and wrote the manuscript. P.J.P. analysed forest extents  
713 and contributed to writing. S.L.L. conceived and managed the AfriTRON forest plot census

714 programme. E.T.A.M. and V.A. helped compare plot data with remote sensing carbon maps. All co-  
715 authors read and approved the manuscript.

716

717 **Competing interests** The authors declare no competing interests.

718

#### 719 **Additional information**

720 Supplementary information is available for this paper at XX (to be added)

721 Correspondence and requests for materials should be addressed to A. C-S.

722 Reprints and permissions information are available at XX (to be added)

723

#### 724 **Data availability**

725 Source data to generate figures and tables are available from:

726 [https://doi.org/10.5521/forestplots.net/2021\\_5](https://doi.org/10.5521/forestplots.net/2021_5)

727

#### 728 **Code availability**

729 R code to generate figures and tables is available from:

730 [https://doi.org/10.5521/forestplots.net/2021\\_5](https://doi.org/10.5521/forestplots.net/2021_5)

731

#### 732 **Affiliations**

733 <sup>1</sup>Department of Environment and Geography, University of York, York, UK. <sup>2</sup>Department of  
734 International Environmental and Development Studies (NORAGRIC), Norwegian University of Life  
735 Sciences, Ås, Norway. <sup>3</sup>Department of Natural Sciences, Manchester Metropolitan University,  
736 Manchester, UK. <sup>4</sup>School of Geography, University of Leeds, Leeds, UK. <sup>5</sup>Climate Change Specialist  
737 Group, Species Survival Commission, International Union for Conservation of Nature, Gland,  
738 Switzerland. <sup>6</sup>University College London, Department of Geography, London, UK. <sup>7</sup>Biology  
739 Department, Université Officielle de Bukavu, Bukavu, DRC. <sup>8</sup>Service of Wood Biology, Royal Museum  
740 for Central Africa, Tervuren, Belgium. <sup>9</sup>Department of Environment, Laboratory of Wood Technology  
741 (Woodlab), Ghent University, Ghent, Belgium. <sup>10</sup>University of Jos, Jos, Nigeria. <sup>11</sup>Nigerian Montane  
742 Forest Project, Taraba State, Nigeria. <sup>12</sup>Department of Geosciences and Geography, University of  
743 Helsinki, Finland. <sup>13</sup>Department of Zoology, Faculty of Science, Charles University, Prague, Czech  
744 Republic. <sup>14</sup>Institute of Vertebrate Biology, Czech Academy of Sciences, Brno, Czech Republic.  
745 <sup>15</sup>Institute of Botany of the Czech Academy of Science, Třeboň, Czech Republic. <sup>16</sup>College of Natural  
746 and Computational Science, Addis Ababa University, Addis Ababa, Ethiopia. <sup>17</sup>Department of Natural  
747 Resource Management, College of Agriculture and Natural Resource, Wolkite University, Wolkite,  
748 Ethiopia. <sup>18</sup>European Commission, Joint Research Centre, Ispra, Italy. <sup>19</sup>UK Centre for Ecology &  
749 Hydrology, Edinburgh, UK. <sup>20</sup>Université du Cinquantenaire Lwiro, Département de sciences de  
750 l'environnement, Kabare, Suk-Kivu, DRC. <sup>21</sup>Isotope Bioscience Laboratory (ISOFYS), Ghent University,  
751 Ghent, Belgium. <sup>22</sup>Plant Systematic and Ecology Laboratory, Higher Teachers' Training College,  
752 University of Yaoundé I, Yaoundé, Cameroon. <sup>23</sup>Institute of Tropical Forest Conservation, Mbarara  
753 University of Science and Technology, Uganda. <sup>24</sup>Biodiversity and Landscape Unit, Gembloux Agro-  
754 Bio Tech, Université de Liège, Liège, Belgium. <sup>25</sup>Institut for Geography, Friedrich-Alexander-  
755 Universität, Erlangen-Nürnberg, Germany. <sup>26</sup>Institut Supérieur d'Agroforesterie et de Gestion de  
756 l'Environnement de Kahuzi-Biega (ISAGE-KB); Département de Eaux et Forêts, Kalehe, DRC. <sup>27</sup>UN  
757 Environment World Conservation Monitoring Center (UNEP-WCMC), Cambridge, UK.  
758 <sup>28</sup>Computational & Applied Vegetation Ecology (CAVELab), Faculty of Bioscience Engineering, Ghent  
759 University, Ghent, Belgium. <sup>29</sup>Department of Anthropology, George Washington University,  
760 Washington DC, USA. <sup>30</sup>School of Life Sciences, University of KwaZulu-Natal, Scottsville,  
761 Pietermaritzburg, South Africa. <sup>31</sup>Shaanxi Key Laboratory for Animal Conservation, Northwest  
762 University, Xi'an, China. <sup>32</sup>International Centre of Biodiversity and Primate Conservation, Dali  
763 University, Dali Yunnan, China. <sup>33</sup>University of Canterbury, New Zealand. <sup>34</sup>Inventory & Monitoring  
764 Program, National Park Service, Fredericksburg, USA. <sup>35</sup>University of Ghent, Belgium. <sup>36</sup>World

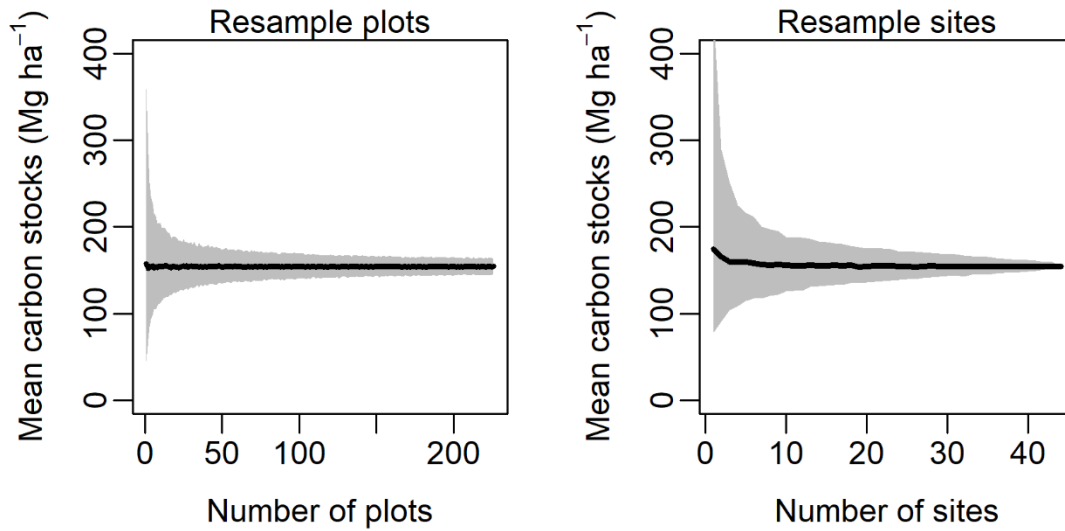
765 Agroforestry (ICRAF), Nairobi, Kenya. <sup>37</sup>Laboratory of Geo-Information Science and Remote Sensing,  
766 Wageningen University, Wageningen, the Netherlands. <sup>38</sup>Geography, Environment & Geomatics,  
767 University of Guelph, Canada. <sup>39</sup>Faculty of Science, University of South Bohemia, České Budějovice,  
768 Czech Republic. <sup>40</sup>AMAP Lab, Université de Montpellier, IRD, CNRS, INRAE, CIRAD, Montpellier,  
769 France. <sup>41</sup>Faculté de Gestion de Ressources Naturelles Renouvelables, Université de Kisangani,  
770 Kisangani, DRC. <sup>42</sup>College of Development Studies, Addis Ababa University, Ethiopia.  
771 <sup>43</sup>Dendrochronology Laboratory, World Agroforestry Centre (ICRAF), Kenya. <sup>44</sup>Missouri Botanical  
772 Garden, St. Louis, Missouri, USA. <sup>45</sup>Department of Biology, University of Burundi, Burundi.  
773 <sup>46</sup>Smithsonian Institution Forest Global Earth Observatory (ForestGEO), Smithsonian Tropical  
774 Research Institute, Washington DC, USA. <sup>47</sup>Kunming Institute of Botany, Kunming, China. <sup>48</sup>Université  
775 Libre de Bruxelles, Brussels, Belgium. <sup>49</sup>Division of Vertebrate Zoology, Yale Peabody Museum of  
776 Natural History, New Haven, CT, USA. <sup>50</sup>Institute for Atmospheric and Earth System Research, Faculty  
777 of Science, University of Helsinki, Finland. <sup>51</sup>Department of Plant Systematics, University of Bayreuth,  
778 Germany. <sup>52</sup>Institute for Geography, Friedrich-Alexander-University Erlangen-Nuremberg, Germany.  
779 <sup>53</sup>Helmholtz-Centre for Environmental Research (UFZ), Leipzig, Germany. <sup>54</sup>Department of Ecology,  
780 Faculty of Science, Charles University, Prague, Czech Republic. <sup>55</sup>International Gorilla Conservation  
781 Programme, Musanze, Rwanda. <sup>56</sup>Department of Natural Resources, Karatina University, Kenya.  
782 <sup>57</sup>Dept. Ecosystem Science & Sustainability, Colorado State University, Fort Collins, USA.  
783 <sup>58</sup>Eco2librium LLC, Boise, USA. <sup>59</sup>Department of Ecology, Université de Kisangani, Kisangani, DRC.  
784 <sup>60</sup>Environmental Change Institute, School of Geography and the Environment, University of Oxford,  
785 Oxford, UK. <sup>61</sup>Tropical Forests and People Research Centre, University of the Sunshine Coast,  
786 Australia. <sup>62</sup>Flamingo Land Ltd., North Yorkshire, UK. <sup>63</sup>College of African Wildlife Management,  
787 Mweka, Tanzania. <sup>64</sup>School of GeoSciences, University of Edinburgh, UK. <sup>65</sup>Department of Geography  
788 and Environmental Sciences, University of Dundee, Dundee, UK. <sup>66</sup>Independent Botanist, Harare,  
789 Zimbabwe. <sup>67</sup>Department of Horticultural Sciences, Faculty of Applied Sciences, Cape Peninsula  
790 University of Technology, Bellville, South Africa. <sup>68</sup>Biology Department, University of Rwanda,  
791 Rwanda. <sup>69</sup>Department of Biological and Environmental Sciences, University of Gothenburg, Sweden.  
792 <sup>70</sup>Mountains of the Moon University, Fort Portal, Uganda. <sup>71</sup>National Agricultural Research  
793 Organisation, Mbarara Zonal Agricultural Research and Development Institute, Mbarara, Uganda.  
794 <sup>72</sup>School of Biological Sciences, University of Southampton, Southampton, UK. <sup>73</sup>Conservation  
795 Science Group, Department of Zoology, University of Cambridge, Cambridge, UK. <sup>74</sup>State Key  
796 Laboratory of Information Engineering in Surveying, Mapping and Remote Sensing, Wuhan  
797 University, China. <sup>75</sup>Key Biodiversity Areas Secretariat, BirdLife International, Cambridge, UK.  
798 <sup>76</sup>School of Life Sciences, University of Lincoln, UK. <sup>77</sup>Department of Biology, University of Florence,  
799 Sesto Fiorentino, Italy. <sup>78</sup>Tropical Biodiversity Section, Museo delle Scienze, Trento, Italy. <sup>79</sup>Tropical  
800 Plant Exploration Group (TroPEG) Cameroon. <sup>80</sup>Center for Development Research (ZEF), University of  
801 Bonn, Germany. <sup>81</sup>Conservation and Landscape Ecology, University of Freiburg, Germany. <sup>82</sup>Applied  
802 Biology and Ecology Research Unit, University of Dschang, Dschang, Cameroon. <sup>83</sup>Forest Ecology and  
803 Forest Management Group, Wageningen University, Wageningen, The Netherlands. <sup>84</sup>Water and  
804 Land Resources Center, Addis Ababa University, Addis Ababa, Ethiopia. <sup>85</sup>African Wildlife Foundation  
805 (AWF), Biodiversity Conservation and Landscape Management Program, Simien Mountains National  
806 Park, Debark, Ethiopia. <sup>86</sup>Faculty of Forestry, University of British Columbia, Vancouver, Canada.  
807 <sup>87</sup>Center for International Forestry Research (CIFOR), Bogor, Indonesia. <sup>88</sup>Department of Forest  
808 Ecology, Faculty of Forestry and Wood Sciences, Czech University of Life Sciences, Prague, Czech  
809 Republic. <sup>89</sup>Department of Plant Biology, Faculty of Sciences, University of Yaoundé I, Cameroon.  
810 <sup>90</sup>Bioversity International, Yaoundé, Cameroon. <sup>91</sup>UK Research & Innovation, UK. <sup>92</sup>Department of  
811 Geography, National University of Singapore, Singapore. <sup>93</sup>Institute of Forestry and Conservation,  
812 University of Toronto, Toronto, Canada. <sup>94</sup>Biodiversity Foundation for Africa, East Dean, East Sussex,  
813 UK. <sup>95</sup>Forestry Development Authority of the Government of Liberia (FDA), Monrovia, Liberia.  
814 <sup>96</sup>School of Forestry and Environmental Studies, Yale University, New Haven, USA. <sup>97</sup>Department of  
815 Biological Sciences, Florida International University, Florida, USA. <sup>98</sup>School of Natural Sciences,

816 University of Bangor, Bangor, UK. <sup>99</sup>Rothamsted Research, Harpenden, UK. <sup>100</sup>University of Liberia,  
817 Monrovia, Liberia. \*corresponding author: [a.cuni-sanchez@york.ac.uk](mailto:a.cuni-sanchez@york.ac.uk)

818

819 **Extended Data**

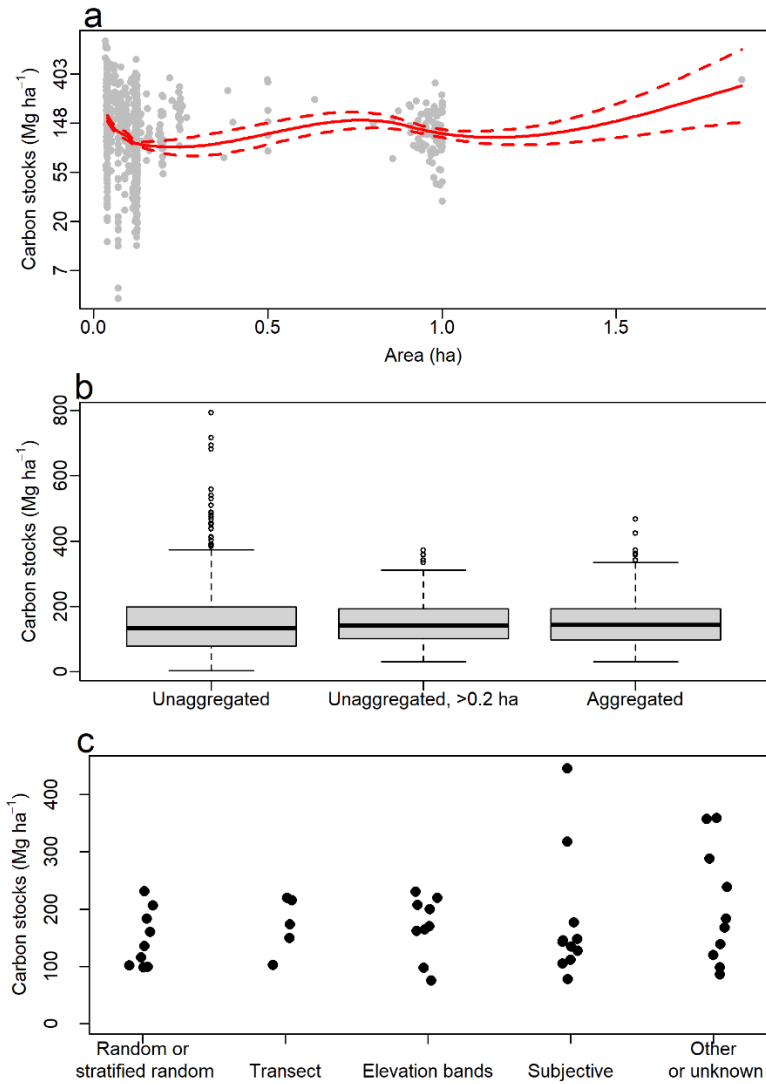
820



821

822 **Extended Data Fig. 1 | Sensitivity of mean aboveground carbon stock estimates to data**  
823 **subsampling.** AfriMont plot data were resampled at different sample sizes either at plot level  
824 (sampling with replacement) or at site level (sampling without replacement).  $N = 1,000$  resamples  
825 for each sample size.

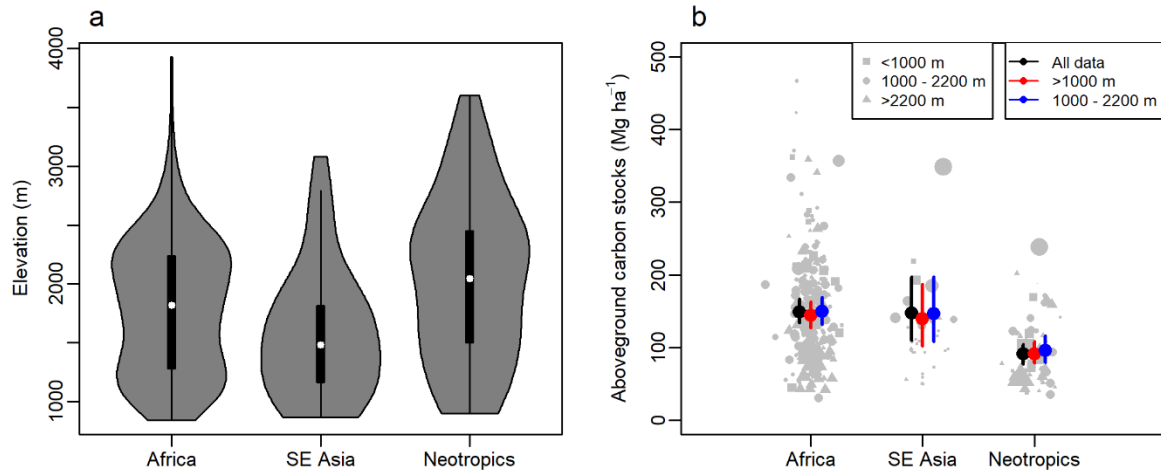
826



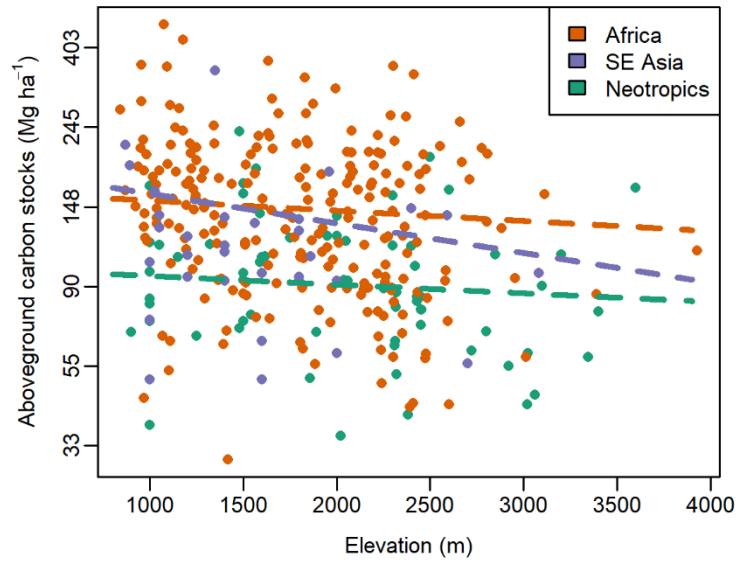
827  
 828 **Extended Data Fig. 2 | Effect of plot area, aggregation procedure and plot design on estimates of**  
 829 **aboveground carbon stocks across the AfriMont plot network. (a)** Relationship between  
 830 aboveground carbon stocks and plot area of plots prior to aggregation. The red line shows the fit of a  
 831 locally weighted regression model (span = 0.75) relating these variables, with dashed lines showing  
 832 the standard errors. **(b)** Variation in aboveground carbon stocks using either all plots prior to  
 833 aggregation (unaggregated), plots prior to aggregation but excluding those < 0.2 ha (unaggregated, >  
 834 0.2 ha) or the aggregated plots used in the main analyses (aggregated). **(c)** Effects of plot design on  
 835 aboveground carbon stocks (each site represents one dot). Sampling strategies include random or  
 836 stratified random, plots positioned along transects, plots established within elevation bands,  
 837 subjective measures such as choosing an area of forest considered representative of the wider area,  
 838 and other strategies (one plot sampled per site or unclear strategy). Carbon stocks (log-transformed)  
 839 did not differ significantly between sites with different sampling strategies (ANOVA:  $F_{4,39} = 0.432$ ,  $P$   
 840 = 0.785). For specific site information see Table S5.

841  
 842

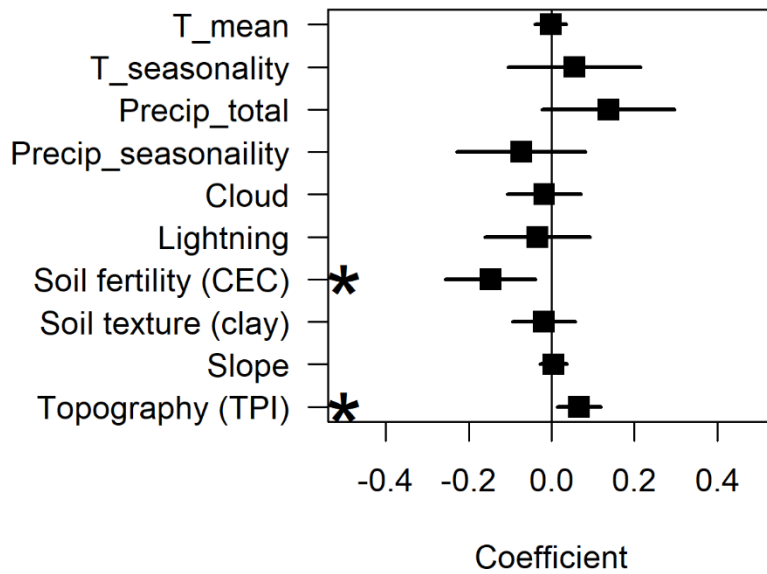




843  
 844 **Extended Data Fig. 3 | Robustness of differences in tropical montane forest aboveground carbon**  
 845 **(AGC) stocks among continents based on plot networks to differences in elevation. (a)** Elevations  
 846 of montane forests plots sampled in each continent. Violin plots show the distribution of data, with  
 847 boxplots showing the median and interquartile range of elevation in each continent. **(b)** Effect of  
 848 removing submontane plots (800-1,000 m asl) and high elevation plots (> 2,200 m asl, approximately  
 849 the upper quartile of elevations for the African montane plot dataset) on AGC-stocks in montane  
 850 forests sampled by plot networks in each continent. Mean AGC-stocks and 95% confidence intervals  
 851 are shown as estimated by models using i) all data, ii) excluding plots 800-1,000 m, and iii) restricting  
 852 plots to 1,000-2,200 m. Means for all plots differ from the analysis in Fig. 1 as literature plots without  
 853 elevation data (plots in Colombia) were excluded from this analysis. Point symbols are proportional  
 854 to square-root plot area.  $N = 324$  plots.  
 855  
 856

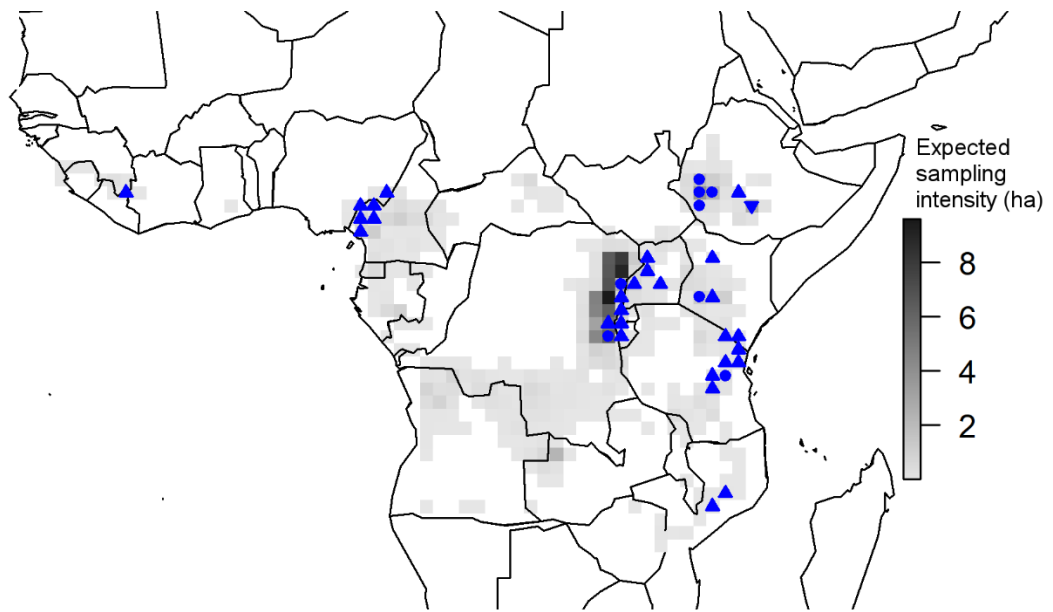


857  
 858 **Extended Data Fig. 4 | Relationship between aboveground carbon (AGC) stocks and elevation for**  
 859 **tropical montane forests in each continent based on plot networks.** Dashed lines show  
 860 relationships from a linear mixed-effects model of log-transformed AGC-stocks as a function of  
 861 elevation, continent and their interaction. Site was included as a random effect, and AGC-stock –  
 862 elevation relationships allowed to vary among sites. Lines show fitted slopes across sites. Neither the  
 863 overall relationship between elevation and AGC-stocks (slope = -0.039 [95% CI = -0.127 – 0.057],  $P =$   
 864 0.420) nor interactions between elevation and continent (Southeast Asia, change in slope = -0.074 [-  
 865 0.294 – 0.149],  $P = 0.503$ ; Neotropics, change in slope = 0.006 [-0.132 – 0.149],  $P = 0.913$ ) are  
 866 statistically significant.  $N = 324$  plots.  
 867  
 868



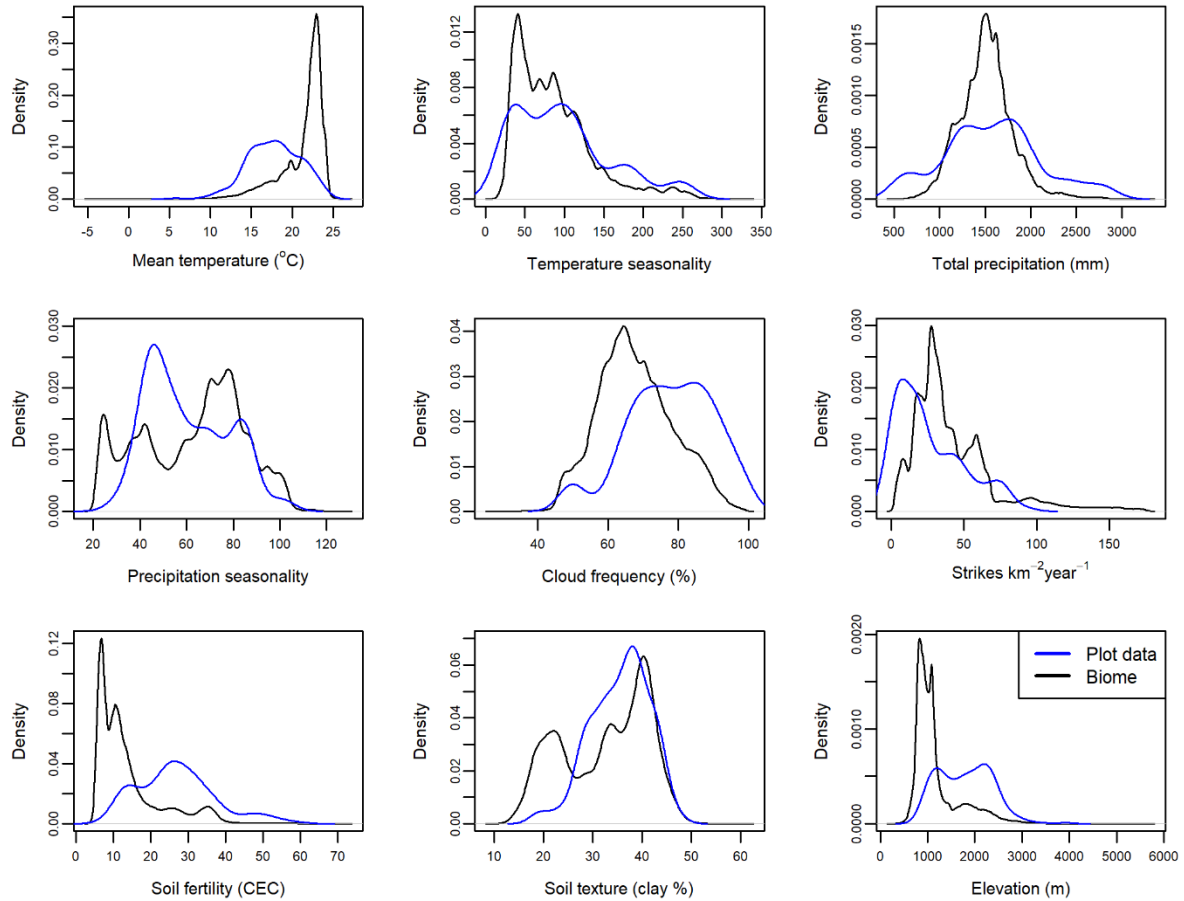
869  
870  
871  
872  
873  
874  
875  
876  
877  
878  
879

**Extended Data Fig. 5 | Environmental drivers of aboveground carbon stocks across the AfriMont plot network.** Coefficients are from a linear mixed-effects model with site as a random intercept. Results are following all-subsets regression and model averaging, in which variables that do not appear in well supported models are given coefficients of zero, leading to shrinkage in model coefficients. Statistically significant relationships ( $P < 0.05$ ) are indicated with asterisks. TPI refers to topographic position index (positive values indicate higher than surroundings, negative values indicate lower than surroundings). T\_mean: annual mean temperature, T\_seasonality: temperature seasonality, Precip\_total: annual precipitation, Precip\_seasonality: precipitation seasonality.



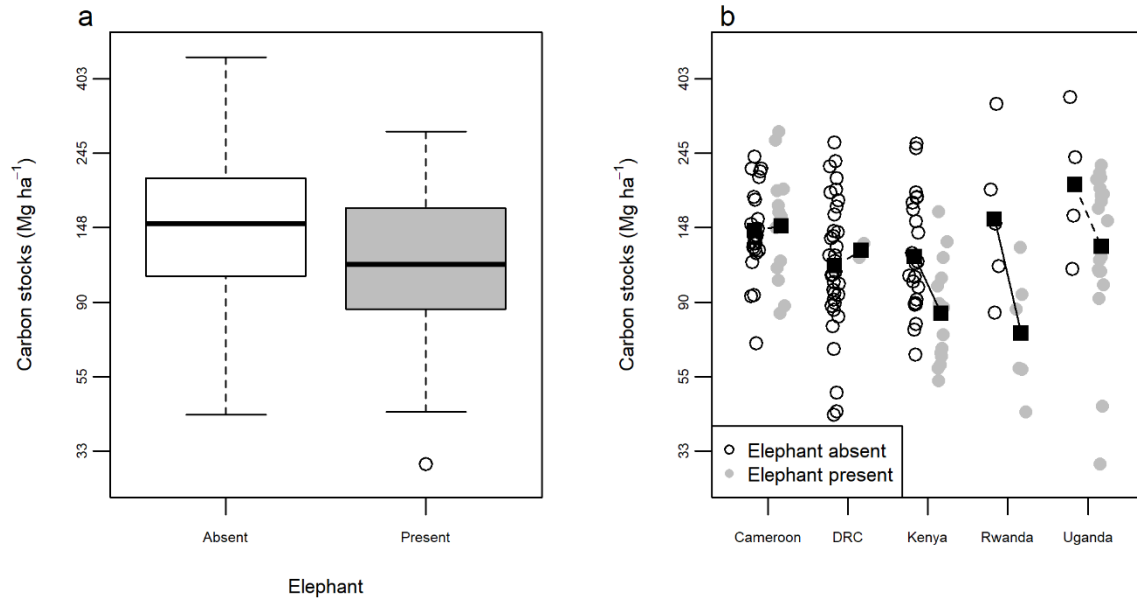
880  
 881  
 882  
 883  
 884  
 885  
 886  
 887  
 888  
 889  
 890

**Extended Data Fig. 6 | Expected sampling effort if effort was distributed in proportion to the area of tropical montane forest biome in Africa.** Data are summarised at 1-degree resolution. Upward triangles show grid-cells where AfriMont sampling effort is more than double expected effort, downward triangles show grid-cells where AfriMont sampling effort is less than half expected effort. Circles denote AfriMont sampling effort being between half and double expected effort. The extent of the tropical montane forest biome was defined as closed-canopy forests  $\geq 800$  m asl in December 2018, extracted from ref.<sup>38</sup> and clipped to 'primary humid forest' using ref.<sup>39</sup>. This grided map differs from Fig. 4 as numerous grids have very little tropical montane forest.



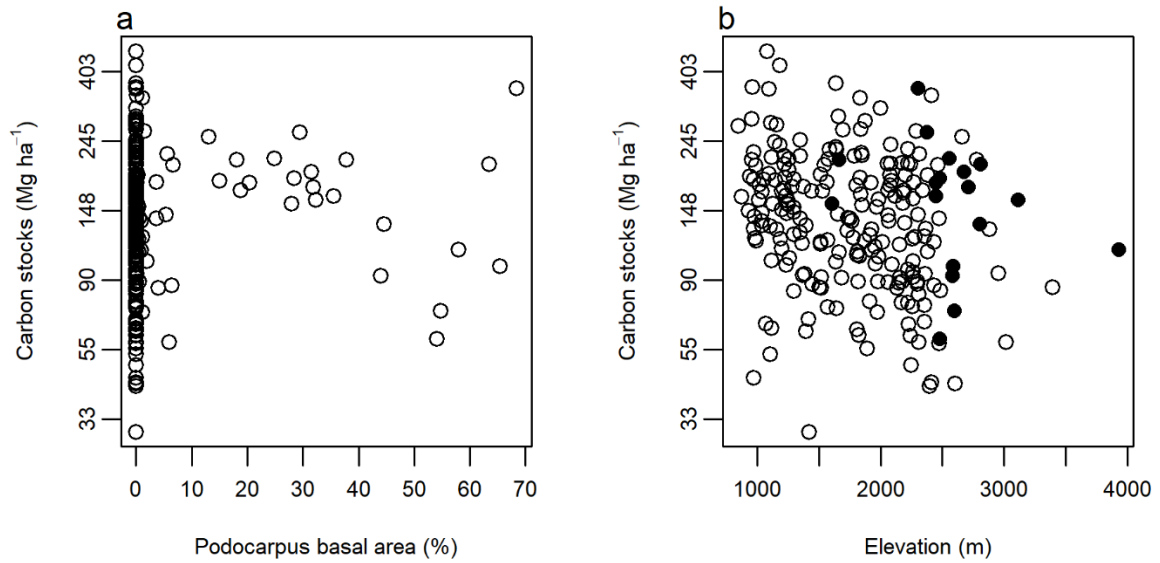
891  
 892 **Extended Data Fig. 7 | Differences in the environmental conditions sampled by the AfriMont plot**  
 893 **network and the tropical montane forest biome in Africa.** The extent of the biome was defined as  
 894 closed-canopy forests  $\geq 800\text{m}$  asl in December 2018, extracted from ref.<sup>38</sup> and clipped to 'primary  
 895 humid forest' using ref.<sup>39</sup>. Environmental variables for the biome were extracted at  $\sim 1\text{-km}$   
 896 resolution.

897  
 898

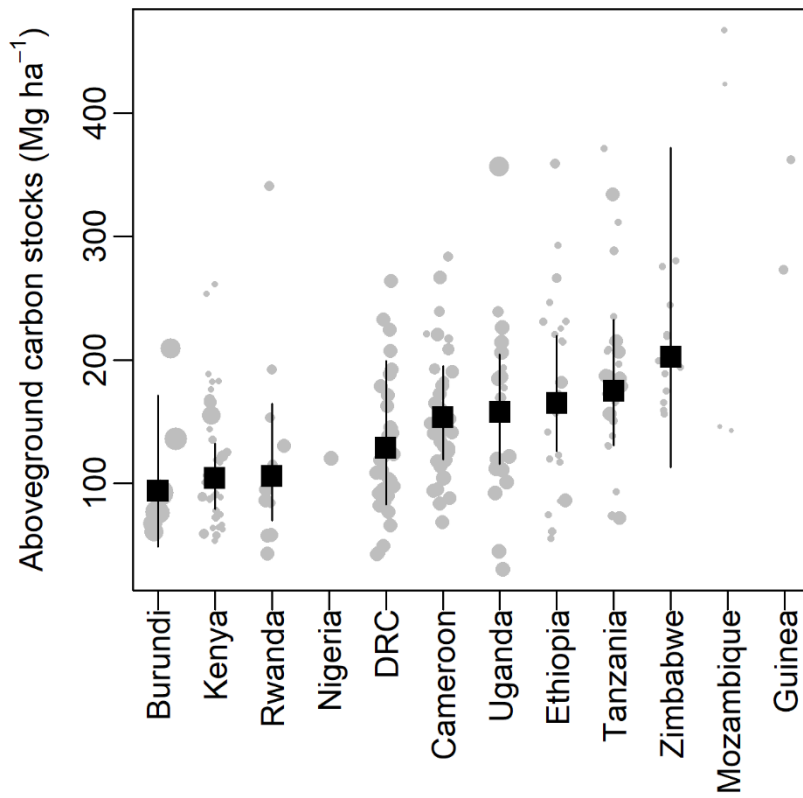


899  
 900  
 901  
 902  
 903  
 904  
 905  
 906  
 907  
 908  
 909

**Extended Data Fig. 8 | Differences in aboveground carbon (AGC) stocks in AfriMont plots located in montane forests with and without elephants.** **a)** Differences across all plots. AGC-stocks are statistically significantly lower in forests with elephants ( $t$ -test,  $t = 3.5$ ,  $df=83.5$ ,  $P = 0.001$ ). The thick line shows the median, and boxes cover the interquartile range (IQR). Values  $> 1.5$  times IQR away from the IQR are shown by points. **b)** Differences in countries where elephants are present in at least one of the montane sites studied. Black squares show means in each country in forests with or without elephants – solid lines denote statistically significant differences ( $t$ -tests,  $P < 0.05$ ). Elephant presence in 2019 was estimated by co-authors (see Table S5).



910  
 911 **Extended Data Fig. 9 | Relationship between aboveground carbon (AGC) stocks and**  
 912 **Podocarpaceae.** (a) Relationship between AGC-stocks and Podocarpaceae basal area across plots in  
 913 the AfriMont network, expressed as a percentage of total plot basal area. These variables are not  
 914 significantly correlated ( $r_s = 0.083$ ,  $n = 226$ ,  $P = 0.212$ ). (b) Distribution of plots with at least 20%  
 915 basal area of Podocarpaceae (black points) in relation to elevation and AGC-stocks. AGC-stocks are  
 916 not significantly related to elevation or Podocarpaceae basal area (Linear mixed effects model,  $P =$   
 917  $0.152$  and  $0.132$  respectively).  
 918  
 919



921 **Extended Data Fig. 10 | Within country variation in aboveground carbon stocks based on the**  
 922 **AfriMont plot network.** Error bars show means and 95% confidence intervals estimated by linear  
 923 mixed-effects models. Modelled means not shown for countries with fewer than five plots. Point size  
 924 is proportional to plot area.  
 925  
 926  
 927  
 928